WP6: graphene spintronics

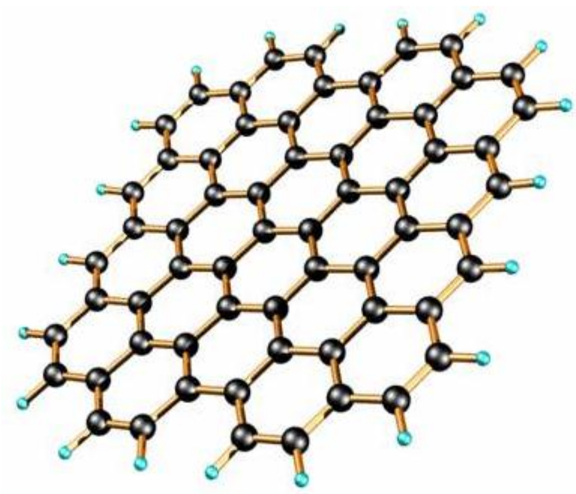

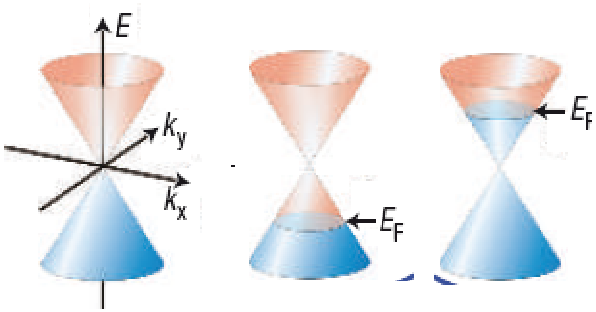

University of Groningen (B. van Wees, WP leader)

Catalan Inst. of Nanosc. and Nanotech. in Barcelona (S.Roche, WP deputy and O. Valenzuela)

Aachen University – RWTH (B. Beschoten)

Basel University (C. Schönenberger)

CSIC Madrid (P. Guinea)

Université catholique de Louvain (J.C. Charlier)

University of Manchester (I. Grigorieva)

University of Regensburg (J. Fabian)

CEA/CNRS/Spintec and CEA/INAC à Grenoble (M. Chshiev, X. Waintal, L. Vila)

UMR CNRS/Thales à Palaiseau (A. Fert, P. Seneor)

Research directions with graphene (roadmap in the Flagship proposal)

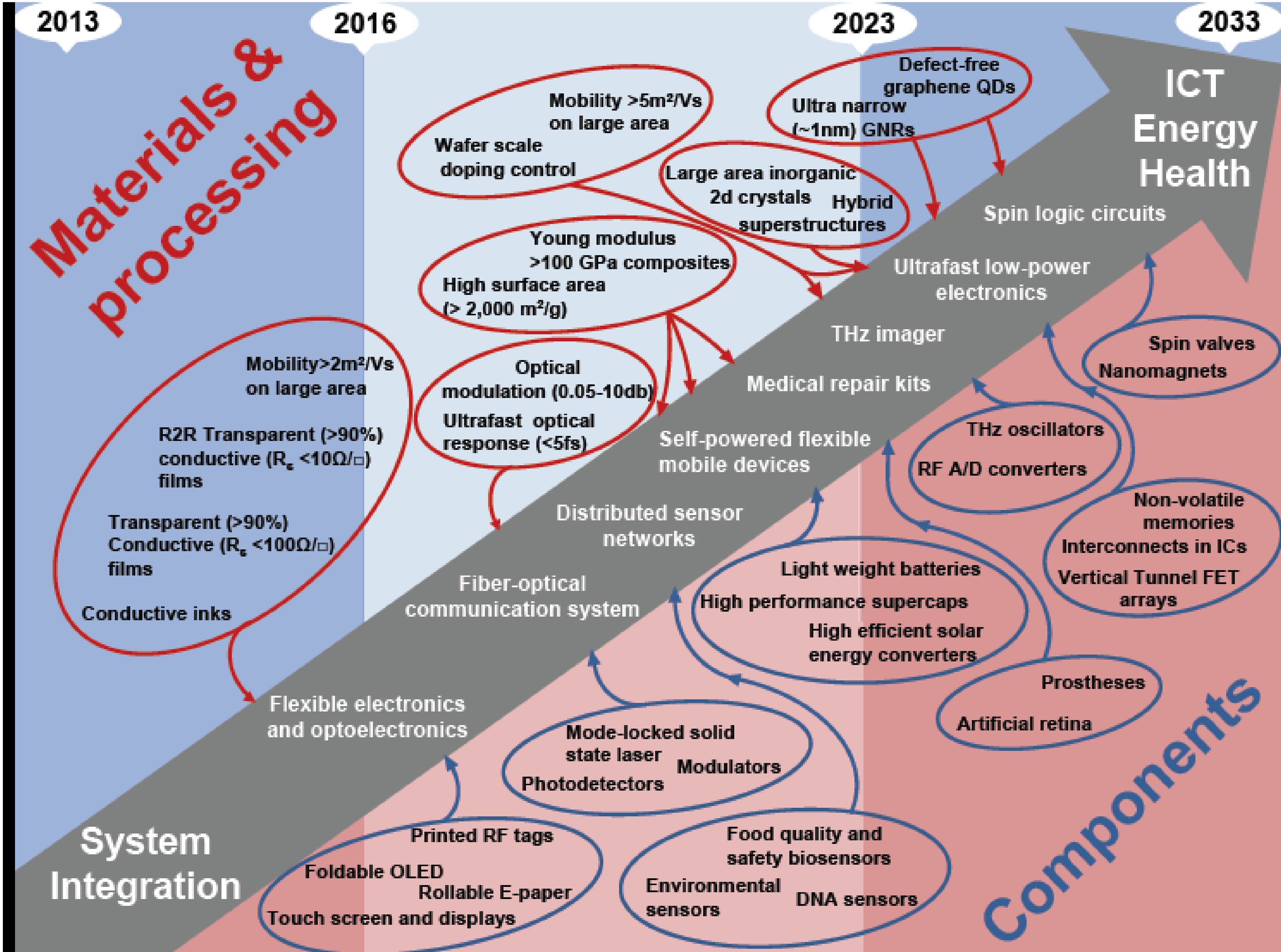

Research directions with graphene (roadmap in the Flagship proposal)

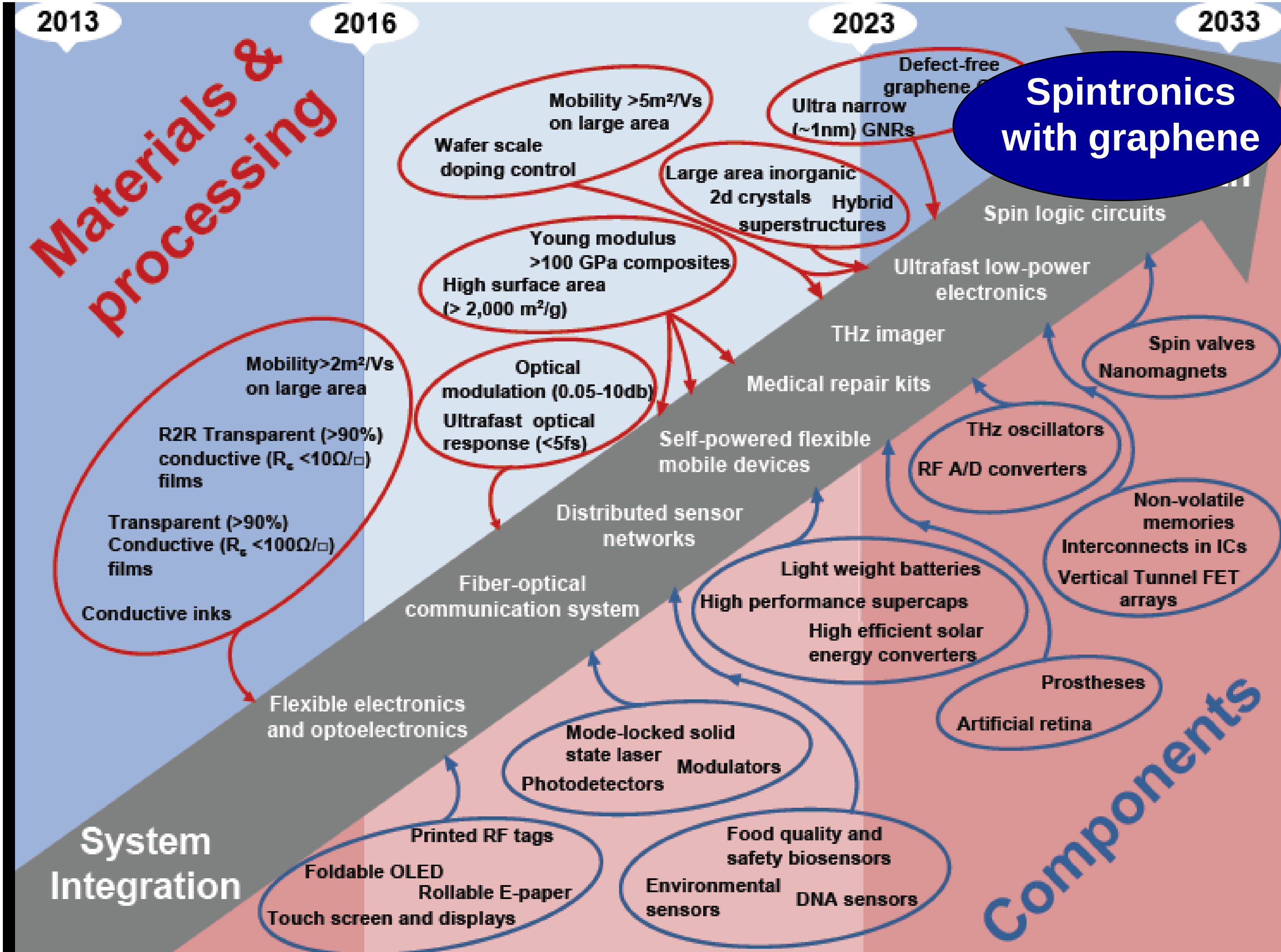

Spintronics, prospects for tomorrow

2011 edition of ITRS (International Tech. Roadmap for Semiconductors)

Emerging Research Devices Section

6.5 Memory and Logic Technologies for Accelerated Development

– STT-RAM is one the 3 technologies to be developed in an accelerated way (to replace RAM or MRAM with advantages in terms of bit density,power dissipation, CMOS integration)

4.2.5 Non-FET, Non Charge-based ‘beyond CMOS’ devices

-*Spin Wave Devices*

-*Nanomagnetic Logic*

- *Spin Torque Logic gate*

-*All Spin Logic*

} 4 spintronic technologies among the 6 technologies put forward for non Charge-based ‘beyond CMOS’ devices

Spintronics, prospects for tomorrow

2011 edition of ITRS (International Tech. Roadmap for Semiconductors)

Emerging Research Devices Section

4.2.5 Non-FET, Non Charge-based ‘beyond CMOS’ devices

-*Spin Wave Devices*

-*Nanomagnetic Logic*

- *Spin Torque Logic gate*

-*All Spin Logic*

4 spintronic technologies among the 6 highlighted technologies

«Graphene exhibits spin transport characteristics that surpass those of any other semiconductor studied to date »

(ITRS Emerging Research Materials Section)

Spintronics, prospects for tomorrow

2011 edition of ITRS (International Tech. Roadmap for Semiconductors)

Emerging Research Devices Section

4.2.5 Non-FET, Non Charge-based 'beyond CMOS' devices

-*Spin Wave Devices*

-*Nanomagnetic Logic*

- *Spin Torque Logic gate*

-*All Spin Logic*

4 spintronic technologies among the 6 highlighted technologies

«Graphene exhibits spin transport characteristics that surpass those of anyother semiconductor studied to date »

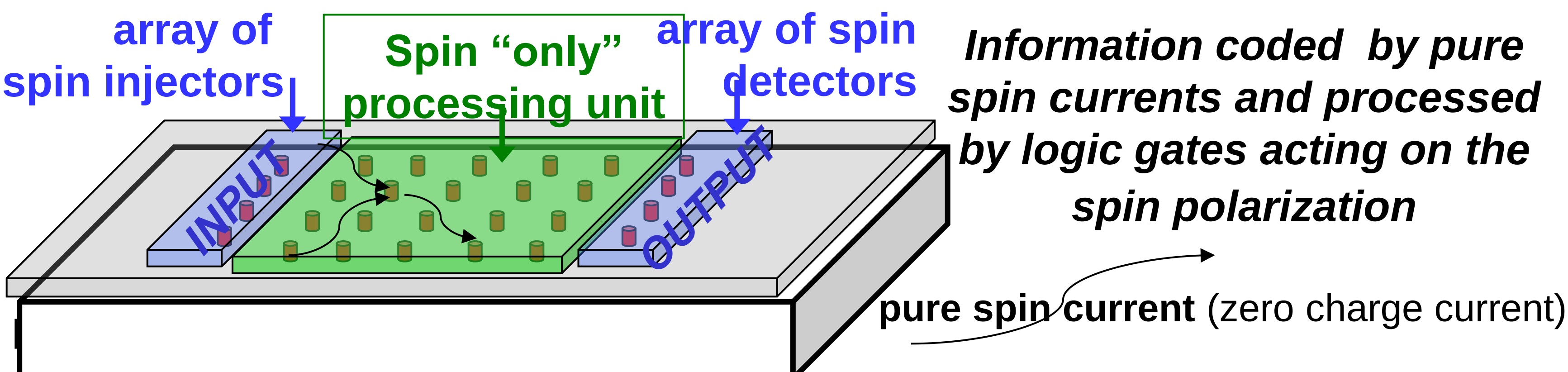

Information coded by pure spin currents and processed by logic gates acting on the spin polarization

Courtesy C. Chappert

Pure spin current

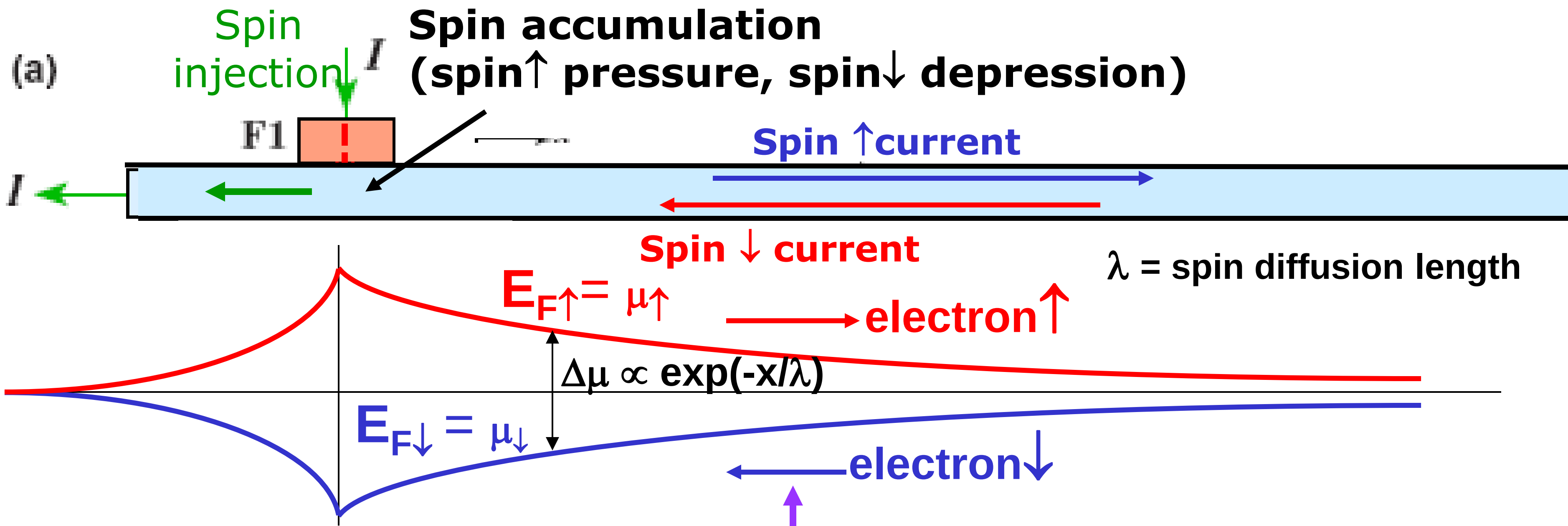

Pure spin current, $J_\uparrow = - J_\uparrow$,
at the right of F1
(no charge current and no capacitance effects)

Pure spin current-based transport and processing of information ?

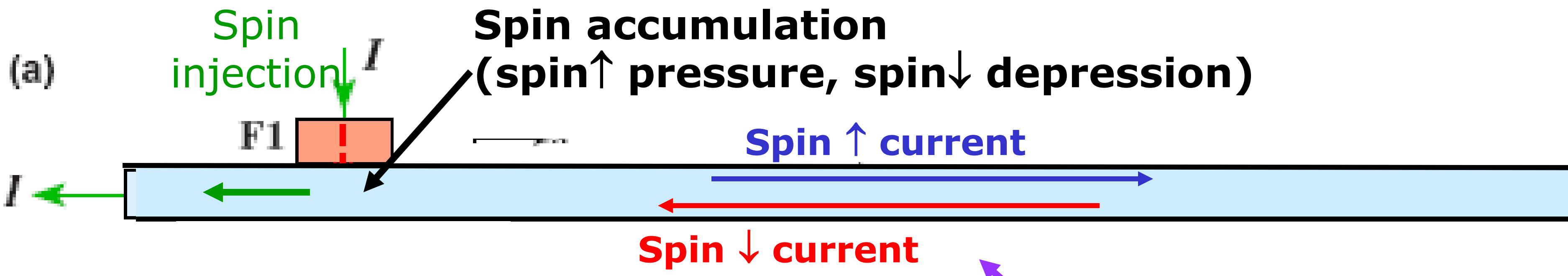

Transport and processing of information (logic gates, etc) coded by the polarization of pure spin currents ?

Pure spin current, $J_{\uparrow} = - J_{\uparrow}$, in N at the right of F1
(no charge current and no capacitance effects)

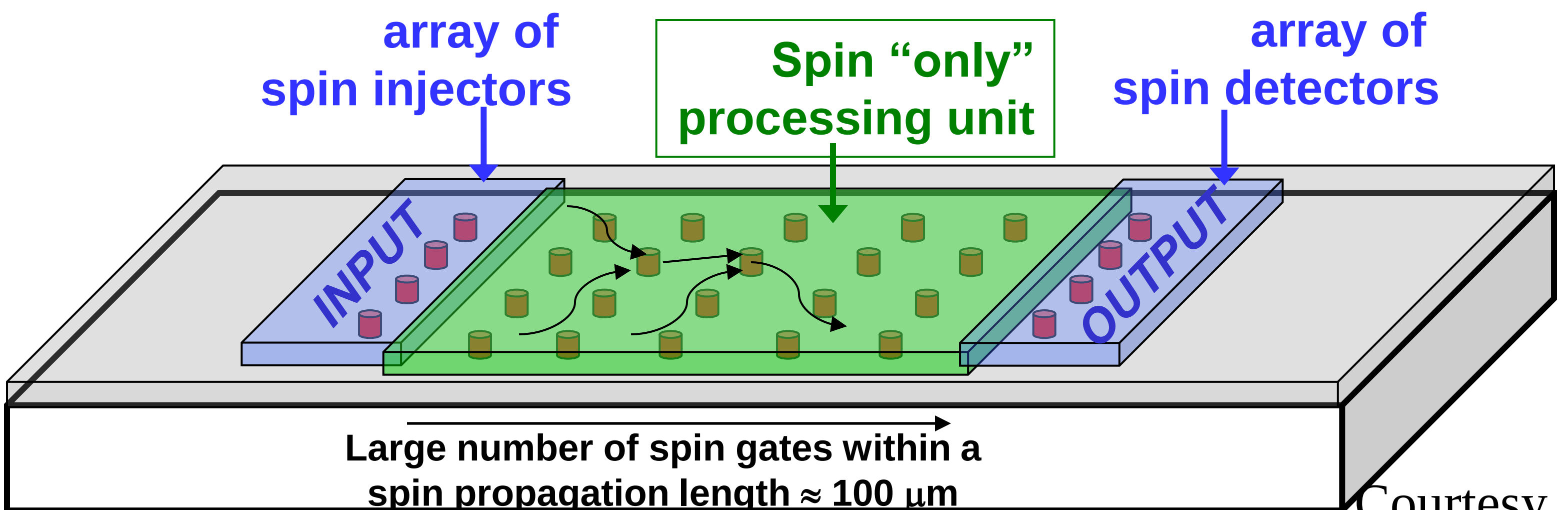

Courtesy C. Chappert

Spintronic logic devices based on spin transport in a lateral channel between spin-polarized electrodes

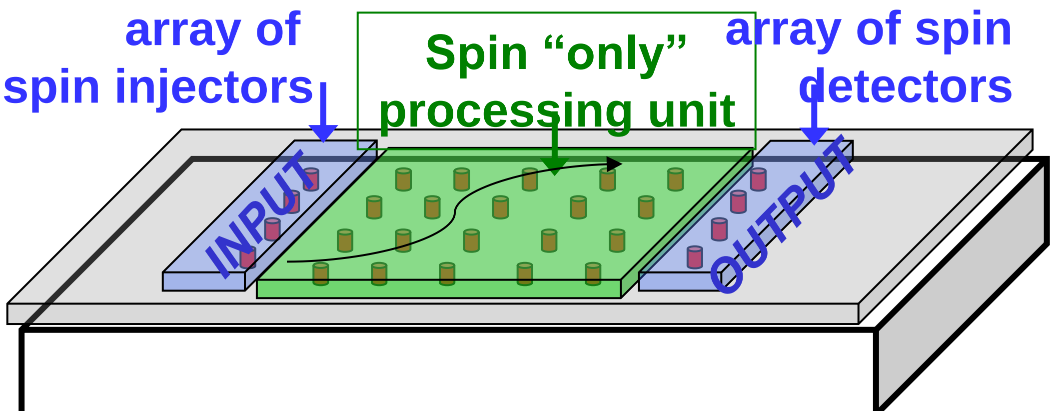

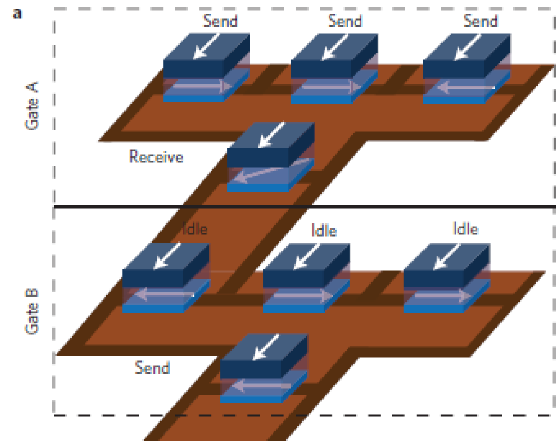

All spin logic with memory
B. Behin-Aein et al, 2010

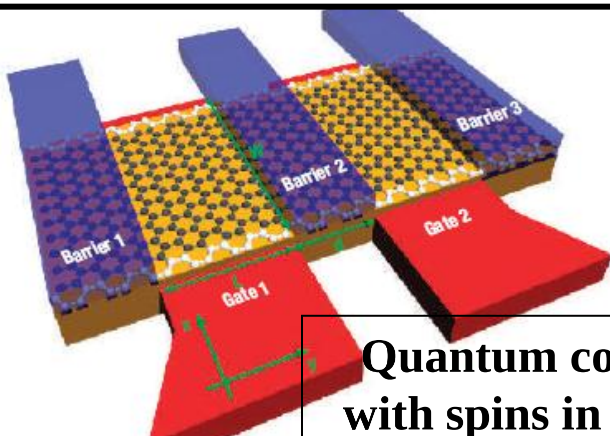

Quantum computing with spins in graphene (Loss et al)

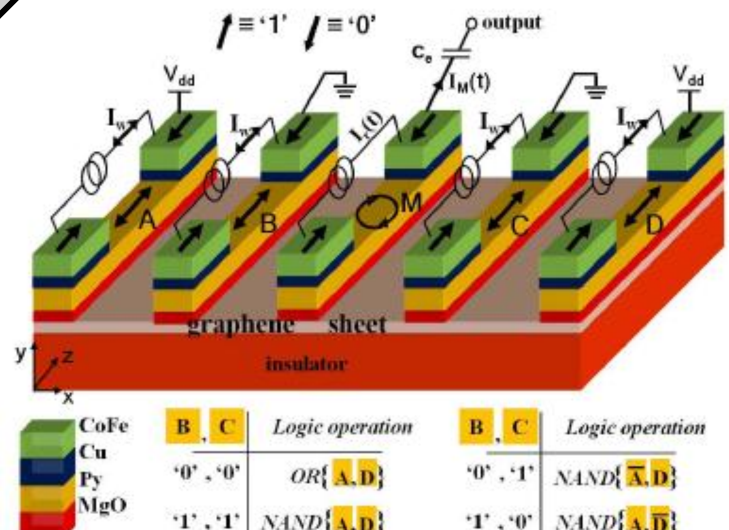

Graphene-based universal logic gate (Dery et al, 2011)

Expected advantges of graphene for spintronic devices

1)* slow spin relaxation *(due to small spin-orbit coupling, ..)

+ large velocity

→long spin diffusion length ≈ 10-100 μm

2) the sensitivity of the electronic properties to adatoms, interfaces, impurities, edges, defects….. can be used

for spin gating

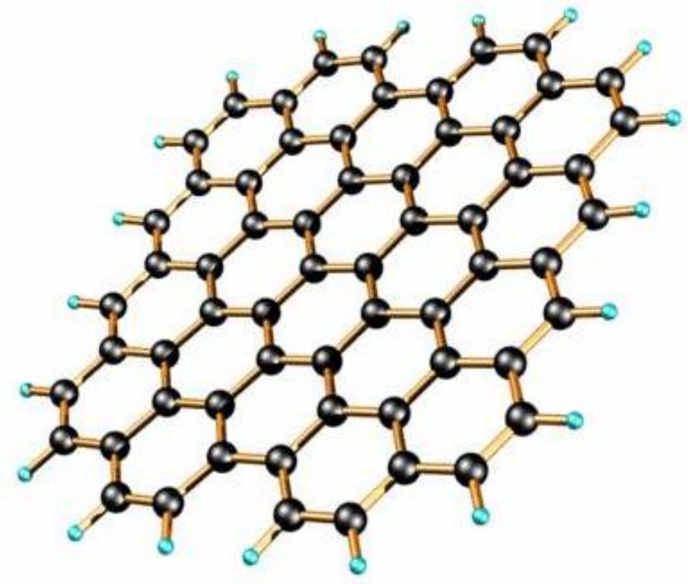

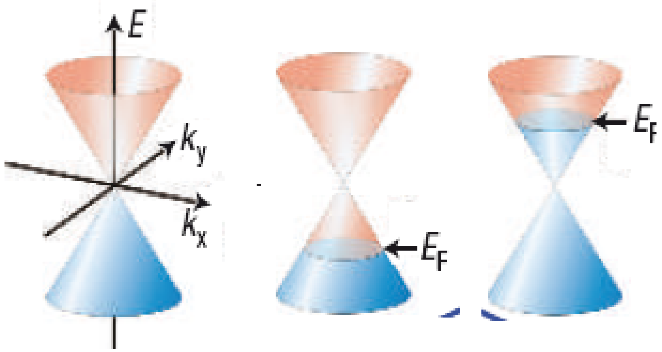

Task 6.1: *Optimizing materials and devices for graphene spintronics* [**RUG**, CNRS, RWTH, ICN, UREG, UBAS]

Task 6.2: *Magnetism in graphene and its interaction with spin transport* [**UMAN**, CNRS, UBAS, RUG, ICN, UCL, CEA,CSIC]

Task 6.3: *Spin transport and spin relaxation in low-dimensional graphene devices* [**RWTH**, RUG, UCL, CSIC]

Task 6.4: *Spin sensors and spin gating graphene devices* (**ICN**, UMAN, RUG, CNRS, CEA, UREG)

Task 6.5: *Towards practical graphene spintronic devices* [all partners]

RUG = Groningen, RWTH = Aachen, CSIC = Madrid, UBAS =Basel, UMAN = Manchester, ICN = Barcelona, UCL = Louvain, UREG = Regensburg, CEA = CEA Grenoble, CNRS = CNRS/Thales,

Task 6.1: *Optimizing materials and devices for graphene spintronics* [**RUG**, CNRS, RWTH, ICN, UREG, UBAS]

The objective of this task is to clarify and understand the physical mechanisms which determine the spin relaxation time and spin relaxation length in high quality graphene devices…

Task 6.1: *Optimizing materials and devices for graphene spintronics* [**RUG**, CNRS, RWTH, ICN, UREG, UBAS]

The objective of this task is to clarify and understand the physical mechanisms which determine the spin relaxation time and spin relaxation length in high quality graphene devices…

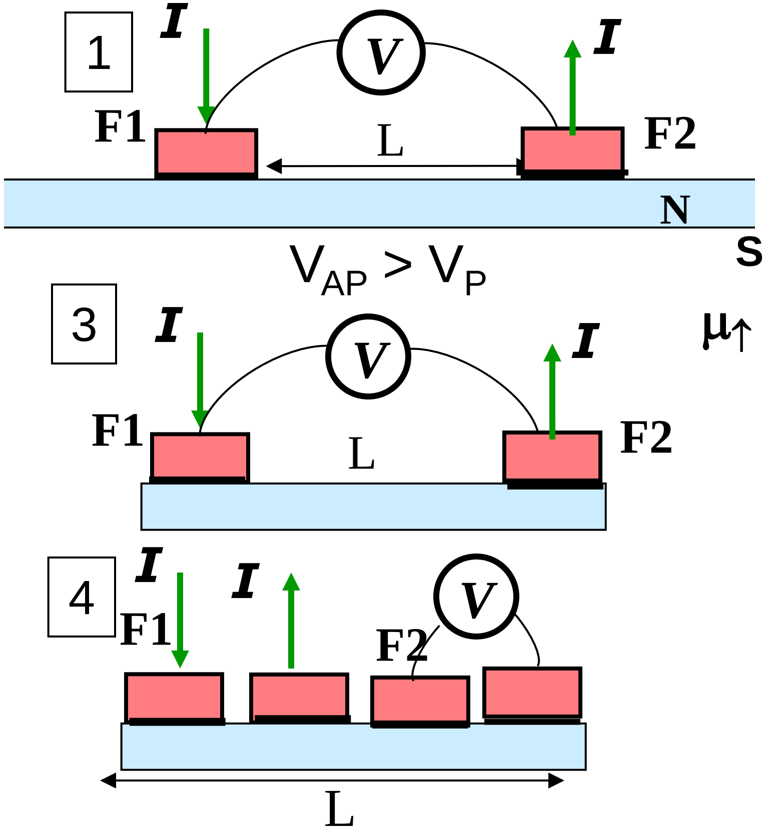

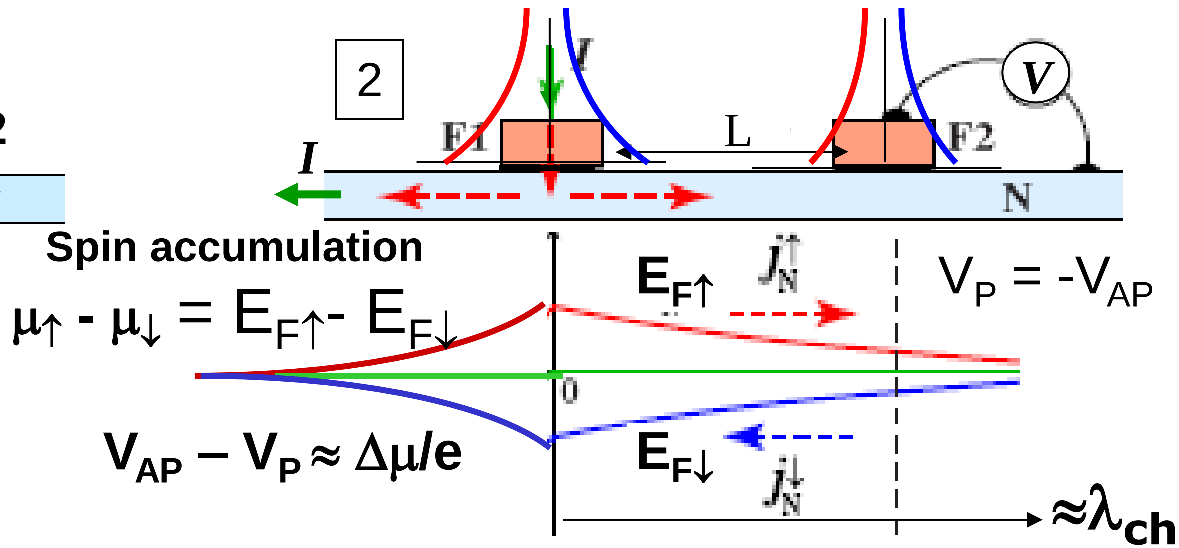

drift/diffusion equations

Localized States Influence Spin Transport in Epitaxial Graphene

T. Maassen,[1,*] J. J. van den Berg,[1] E. H. Huisman,[1] H. Dijkstra,[1] F. Fromm,[2] T. Seyller,[2] and B. J. van Wees[1]
[1]*Physics of Nanodevices, Zernike Institute for Advanced Materials, University of Groningen, Nijenborgh 4, 9747 AG Groningen, The Netherlands*
[2]*Lehrstuhl für Technische Physik, Universität Erlangen-Nürnberg, Erwin-Rommel-Strasse 1, 91058 Erlangen, Germany*
(Received 15 August 2012; published 6 February 2013)

We developed a spin transport model for a diffusive channel with coupled localized states that result in an effective increase of spin precession frequencies and a reduction of spin relaxation times in the system. We apply this model to Hanle spin precession measurements obtained on monolayer epitaxial graphene on SiC(0001). Combined with newly performed measurements on quasi-free-standing monolayer epitaxial graphene on SiC(0001) our analysis shows that the different values for the diffusion coefficient measured in charge and spin transport measurements on monolayer epitaxial graphene on SiC(0001) and the high values for the spin relaxation time can be explained by the influence of localized states arising from the buffer layer at the interface between the graphene and the SiC surface.

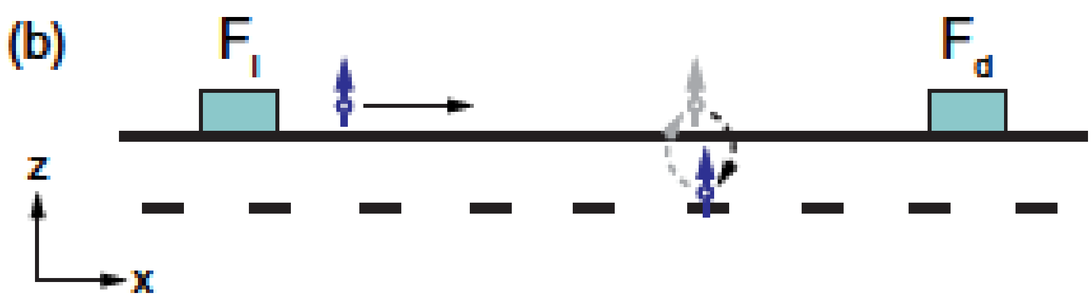

Task 6.1: *Optimizing materials and devices for graphene spintronics* [**RUG**, CNRS, RWTH, ICN, UREG, UBAS]

The objective of this task is to clarify and understand the physical mechanisms which determine the spin relaxation time and spin relaxation length in high quality graphene devices…

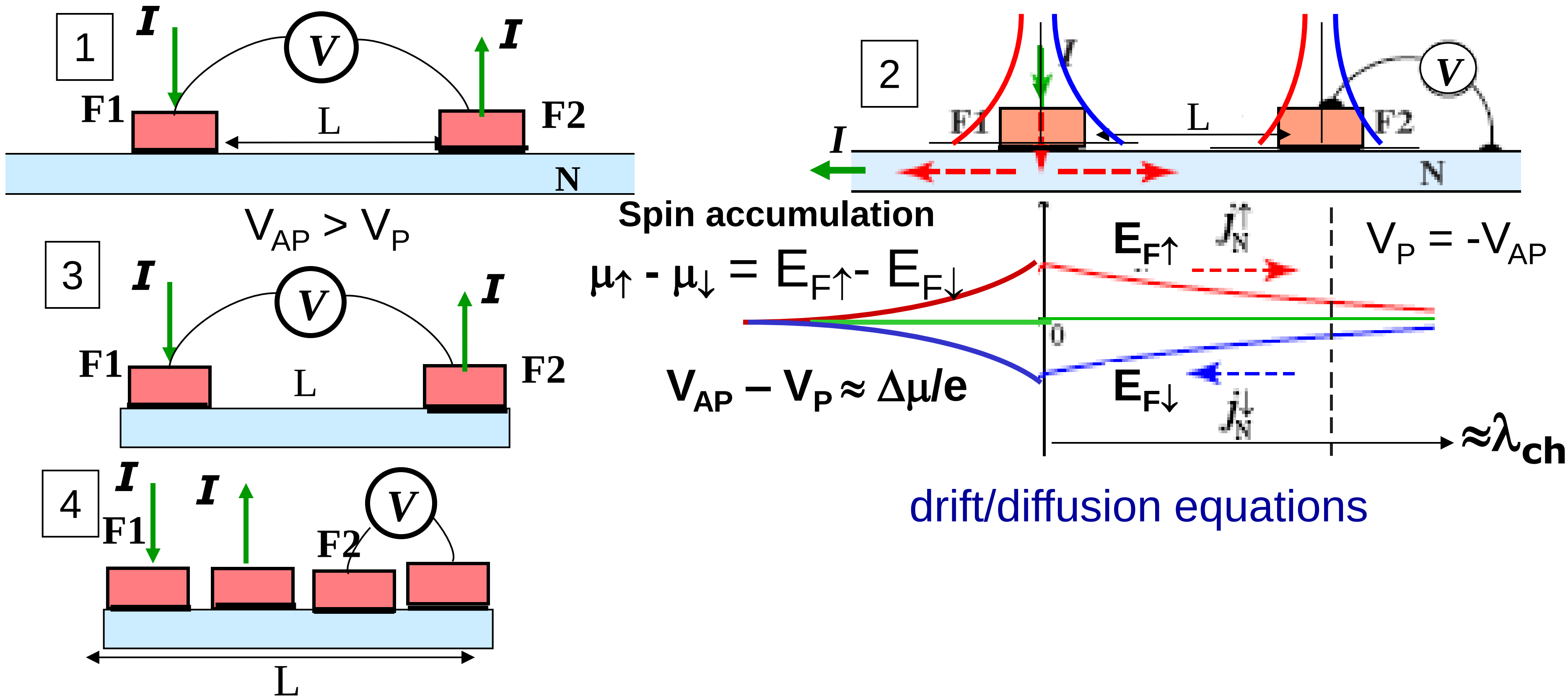

L.Hueso, AF et al, Nature 445, 410, 2007

B. Dlubak et al, Nat. Phys.8, 557, 2012

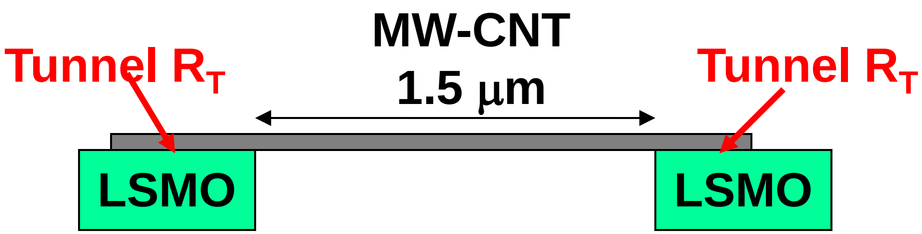

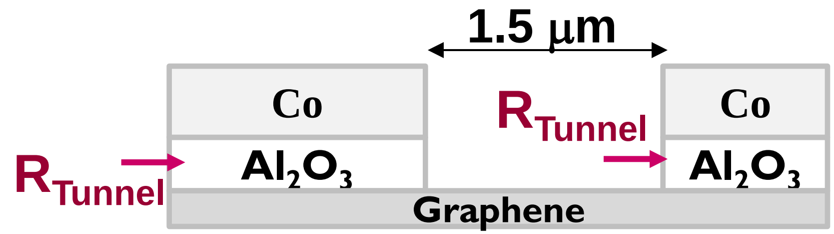

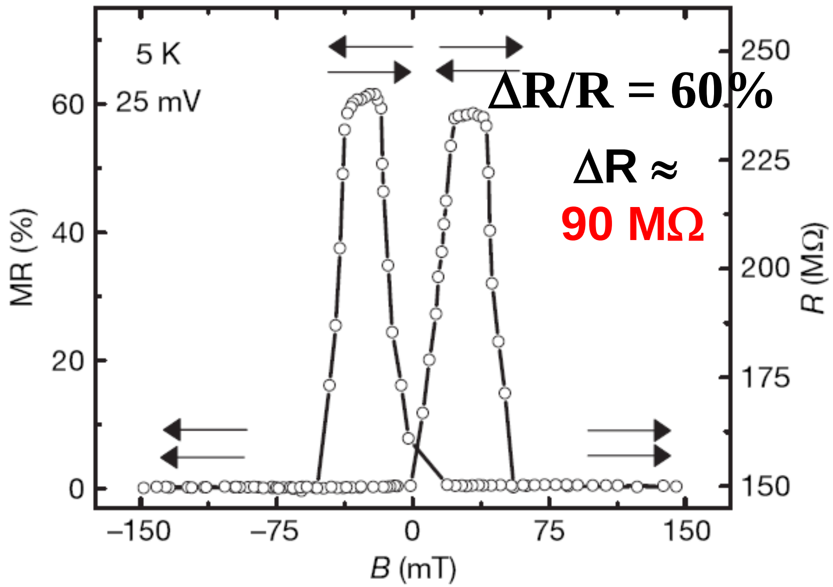

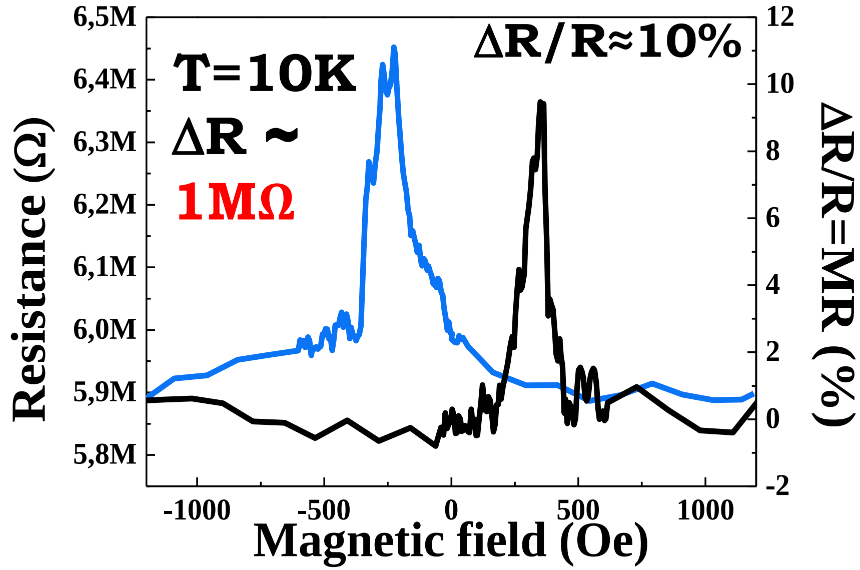

L.Hueso, AF et al, Nature 445, 410, 2007 B. Dlubak et al, Nat. Phys.8, 557, 2012

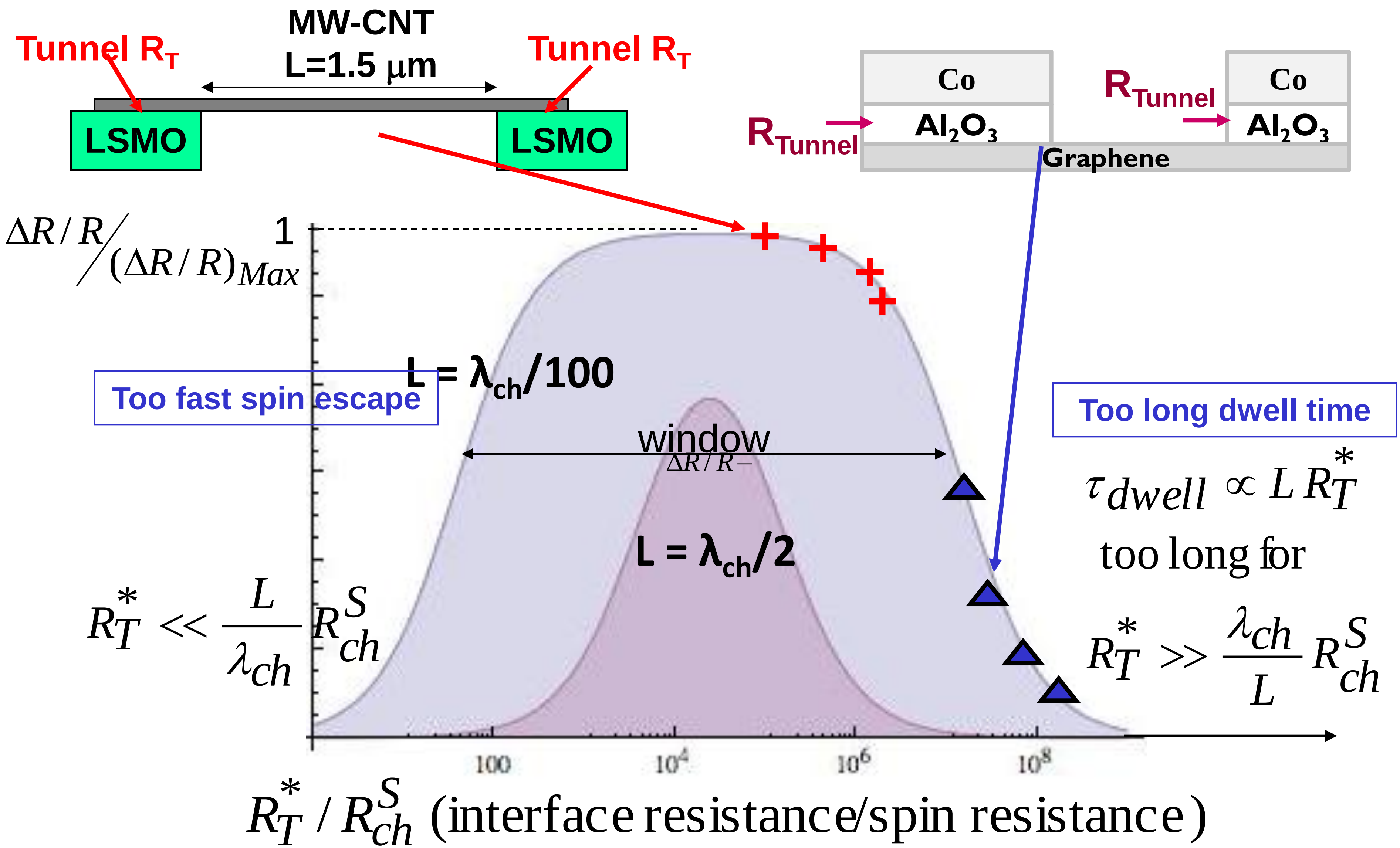

interface ressitance $R_{ch}^S = \rho_{ch} \lambda_{ch}$

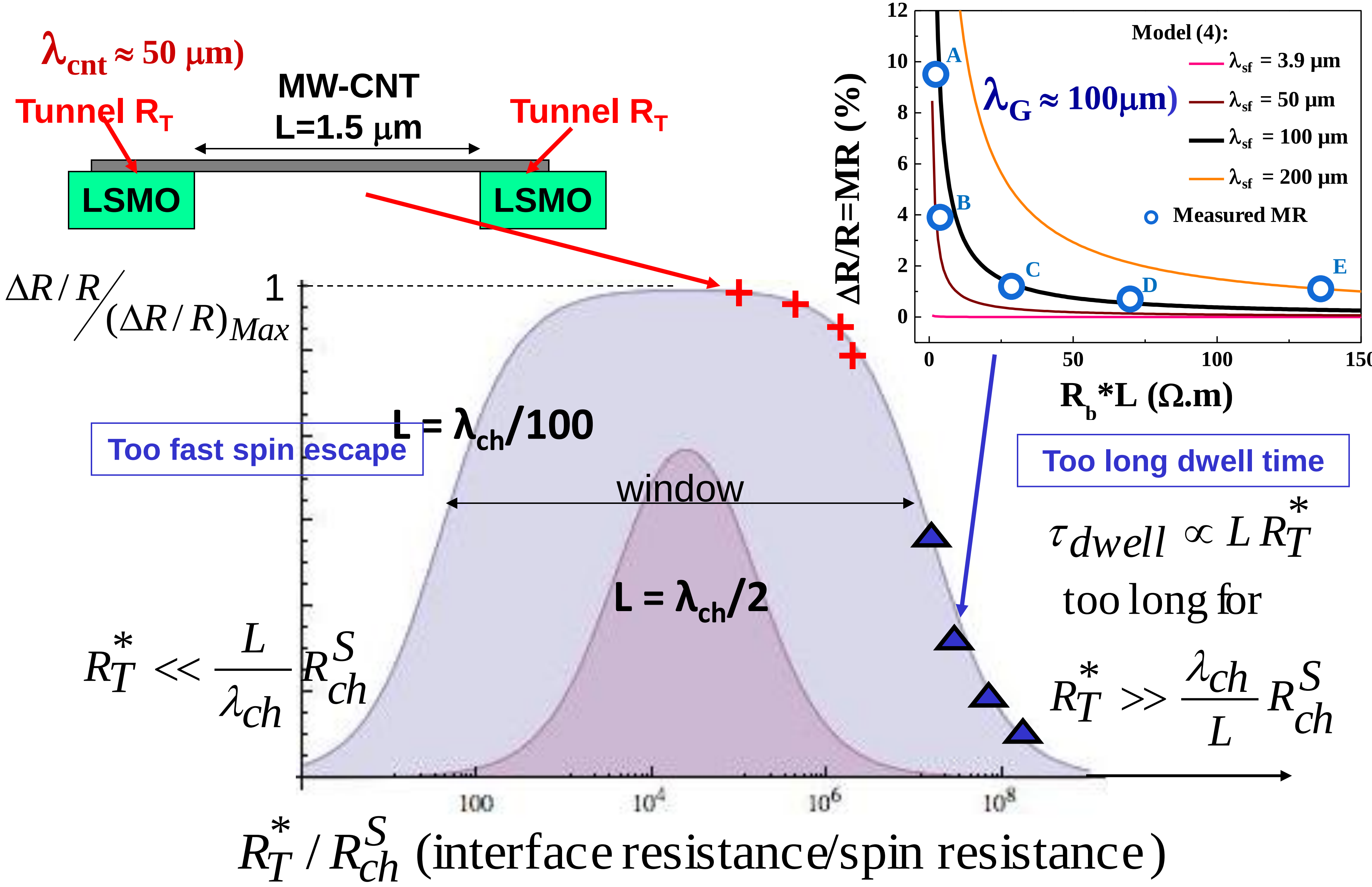

interface ressitance $R_{ch}^{S} = \rho_{ch}\,\lambda_{ch}$

Elliot-Yafet Mechanism in Graphene

H. Ochoa,[1] A. H. Castro Neto,[2,3] and F. Guinea[1]

[1]*Instituto de Ciencia de Materiales de Madrid, CSIC, Sor Juana Inés de la Cruz 3, 28049 Madrid, Spain*
[2]*Graphene Research Centre and Physics Department, National University of Singapore, 2 Science Drive 3, 117542, Singapore*
[3]*Department of Physics, Boston University, 590 Commonwealth Avenue, Boston, Massachusetts 02215, USA*

(Received 18 July 2011; published 17 May 2012)

The differences between spin relaxation in graphene and in other materials are discussed. For relaxation by scattering processes, the Elliot-Yafet mechanism, the relation between the spin and the momentum scattering times, acquires a dependence on the carrier density, which is independent of the scattering mechanism and the relation between mobility and carrier concentration. This dependence puts severe restrictions on the origin of the spin relaxation in graphene. The density dependence of the spin relaxation allows us to distinguish between ordinary impurities and defects which modify locally the spin-orbit interaction.

Functionalization of graphene for spin manipulation (by gate, etc)

Task 6.2: *Magnetism in graphene and its interaction with spin transport* [**UMAN**, CNRS, UBAS, RUG, ICN, UCL, CEA,CSIC]

The objective of this task is to develop spintronic devices with tunable magnetism or spin gating functionality

Task 6.3: *Spin transport and spin relaxation in low-dimensional graphene devices* [**RWTH**, RUG, UCL, CSIC]

This task will explore to which extent (quantum) confinement of carriers affects spin relaxation and spin dephasing.

PHYSICAL REVIEW B 84, 214404 (2011)

Inducing and optimizing magnetism in graphene nanomeshes

Hong-Xin Yang and Mairbek Chshiev*
SPINTEC, CEA/CNRS/UJF-Grenoble 1/Grenoble-INP, INAC, FR-38054 Grenoble, France

Danil W. Boukhvalov
School of Computational Sciences, Korea Institute for Advanced Study (KIAS), Hoegiro 87, Dongdaemun-Gu, Seoul 130-722, Korean Republic

Xavier Waintal
SPSMS-INAC-CEA, 17 rue des Martyrs, FR-38054 Grenoble, France

Stephan Roche
CIN2 (ICN-CSIC) and Universitat Autonoma de Barcelona, Catalan Institute of Nanotechnology, Campus de la UAB, ES-08193 Bellaterra (Barcelona), Spain and ICREA, Institució Catalana de Recerca i Estudis Avancats, ES-08010 Barcelona, Spain

Magnetism and spin splitting induced by vacancies (nanomeshes)

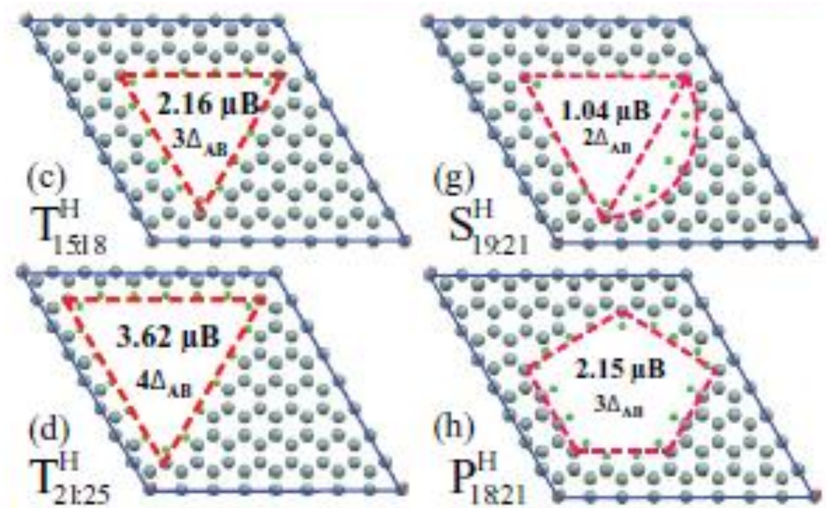

PRL 103, 026804 (2009) PHYSICAL REVIEW LETTERS week endi
10 JULY 2

Spin-orbit effects

Impurity-Induced Spin-Orbit Coupling in Graphene

A. H. Castro Neto[1] and F. Guinea[2]
[1]Department of Physics, Boston University, 590 Commonwealth Avenue, Boston Massachusetts 02215, USA
[2]Instituto de Ciencia de Materiales de Madrid, CSIC, Cantoblanco E28049 Madrid, Spain
(Received 27 February 2009; published 10 July 2009)

We study the effect of impurities in inducing spin-orbit coupling in graphene. We show that the sp^3 distortion induced by an impurity can lead to a large increase in the spin-orbit coupling with a value comparable to the one found in diamond and other zinc-blende semiconductors. The spin-flip scattering produced by the impurity leads to spin scattering lengths of the order found in recent experiments. Our results indicate that the spin-orbit coupling can be controlled via the impurity coverage.

PRL 104, 146801 (2010) PHYSICAL REVIEW LETTERS week ending
9 APRIL 201

Spin filtering

Band Engineering and Magnetic Doping of Epitaxial Graphene on SiC (0001)

Thushari Jayasekera,[1] B. D. Kong,[2] K. W. Kim,[2] and M. Buongiorno Nardelli[1,3,*]
[1]Department of Physics, North Carolina State University, Raleigh, North Carolina 27695-7518, USA
[2]Department of Electrical and Computer Engineering, North Carolina State University, Raleigh, North Carolina 27695-7911, US
[3]Computer Science and Mathematics Division, Oak Ridge National Laboratory, Oak Ridge, Tennessee 37831-6359, USA
(Received 13 December 2009; published 5 April 2010)

Using calculations from first principles we show how specific interface modifications can lead to a fine-tuning of the doping and band alignment in epitaxial graphene on SiC. Upon different choices of dopants, we demonstrate that one can achieve a variation of the valence band offset between the graphene Dirac point and the valence band edge of SiC up to 1.5 eV. Finally, via appropriate magnetic doping one can induce a half-metallic behavior in the first graphene monolayer. These results clearly establish the potential for graphene utilization in innovative electronic and spintronic devices.

Giant Magnetoresistance in Ultrasmall Graphene Based Devices

F. Muñoz-Rojas, J. Fernández-Rossier,* and J. J. Palacios
Departamento de Física Aplicada, Universidad de Alicante, San Vicente del Raspeig, E-03690 Alicante, Spain
(Received 13 November 2008; published 3 April 2009)

By computing spin-polarized electronic transport across a finite zigzag graphene ribbon bridging two metallic graphene electrodes, we demonstrate, as a proof of principle, that devices featuring 100% magnetoresistance can be built entirely out of carbon. In the ground state a short zigzag ribbon is an antiferromagnetic insulator which, when connecting two metallic electrodes, acts as a tunnel barrier that suppresses the conductance. The application of a magnetic field makes the ribbon ferromagnetic and conductive, increasing dramatically the current between electrodes. We predict large magnetoresistance in this system at liquid nitrogen temperature and 10 T or at liquid helium temperature and 300 G.

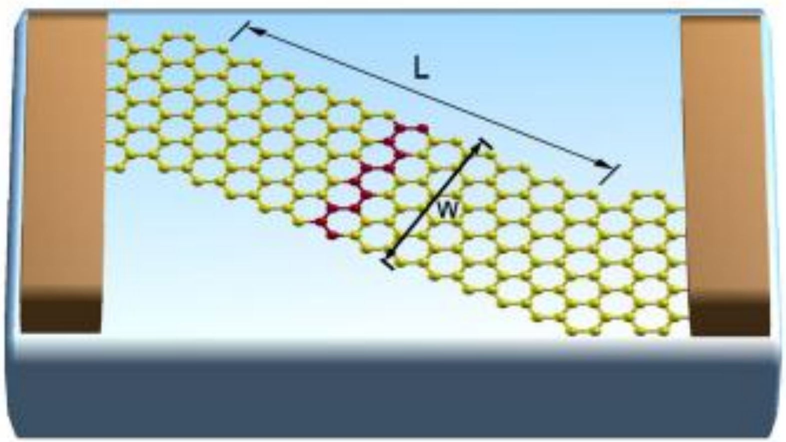

FIG. 1 (color online). Atomic structure of the zigzag ribbon with length $N_x = 12$ and width $N_y = 6$ attached to semi-infinite electrodes. The unit cell of a zigzag ribbon is highlighted.

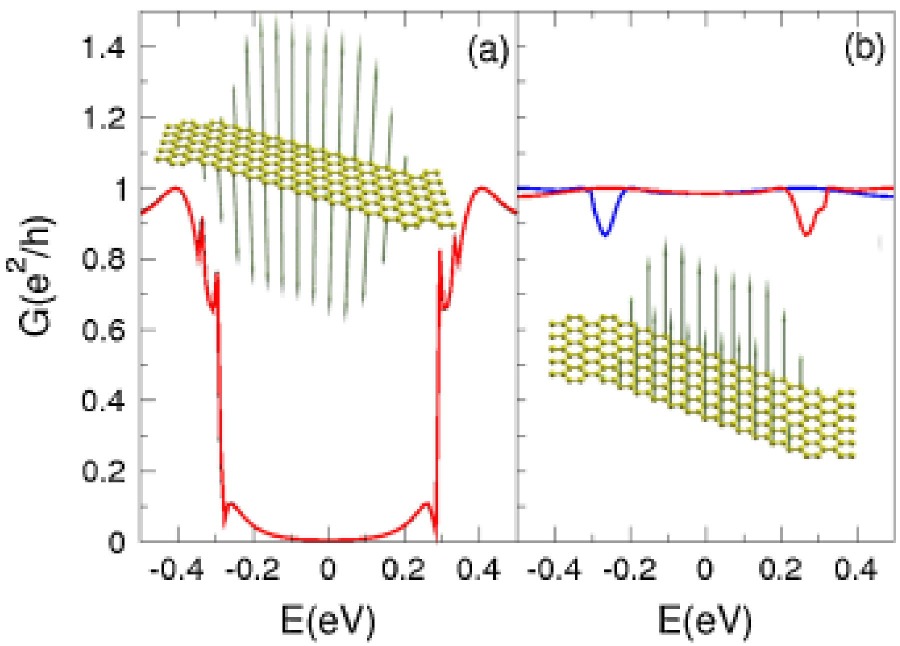

FIG. 3 (color online). (a) Spin resolved transmission for the AF infinite ribbon with $N_x = 12$ and $N_y = 6$. (b) Same for the FM solution. Insets: self-consistently calculated local spin density.

PRL 102, 136810 (2009)

Task 6.4: *Spin sensors and spin gating graphene devices* (**ICN**, UMAN, RUG, CNRS, CEA, UREG)

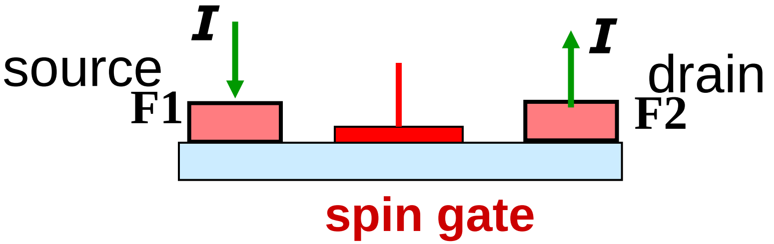

Task 6.5: *Towards practical graphene spintronic devices* [all partners]

Task 6.1: *Optimizing materials and devices for graphene spintronics* [**RUG**, CNRS, RWTH, ICN, UREG, UBAS]

Task 6.2: *Magnetism in graphene and its interaction with spin transport* [**UMAN**, CNRS, UBAS, RUG, ICN, UCL, CEA,CSIC]

Task 6.3: *Spin transport and spin relaxation in low-dimensional graphene devices* [**RWTH**, RUG, UCL, CSIC]

Task 6.4: *Spin sensors and spin gating graphene devices* (**ICN**, UMAN, RUG, CNRS, CEA, UREG)

Task 6.5: *Towards practical graphene spintronic devices* [all partners]

RUG = Groningen (700 kE), RWTH = Aachen (500 kE), CSIC = Madrid (150 kE), UBAS = Basel (350 kE),, UMAN = Manchester (350 kE), ICN = Barcelona (550 kE), UCL = Louvain (250 kE), UREG = Regensburg (500 kE), CEA = CEA Grenoble (250 kE), CNRS = CNRS/Thales (600 kE),

Merci pour votre attention

Interpretation, determination of spin lifetimes and diffusion lengths

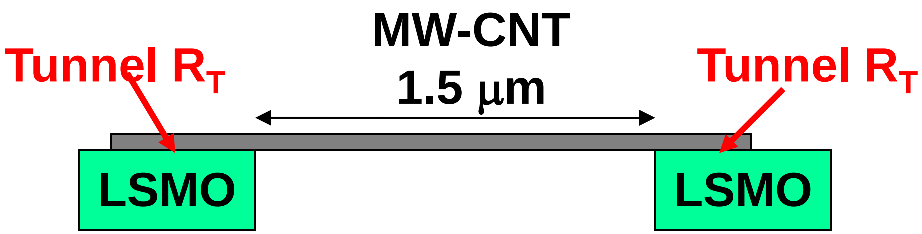

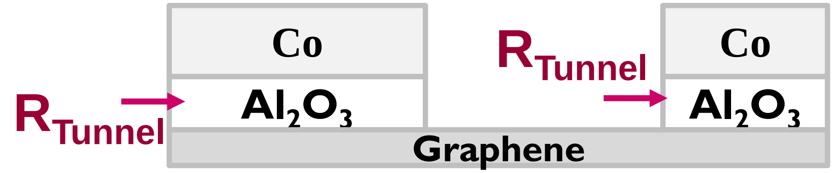

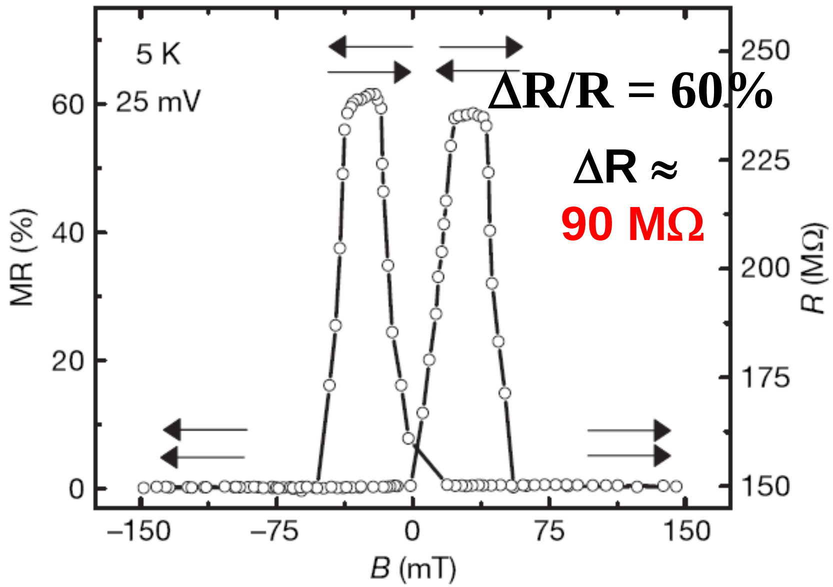

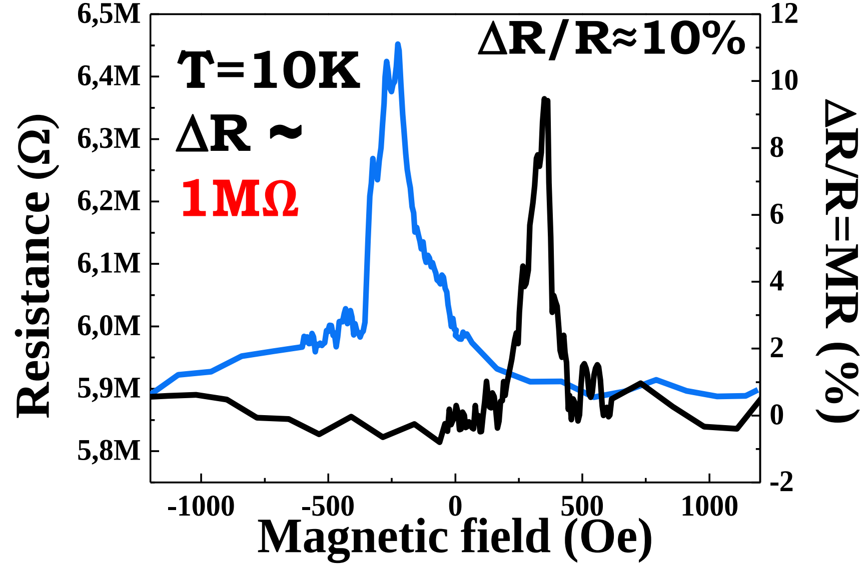

Next stages for graphene

1) Understanding of spin relaxation in graphene (see Ochoa-Guinea, PRL 2012) and lengthening of the spin diffusion length

2) Spin manipulation by gate ?

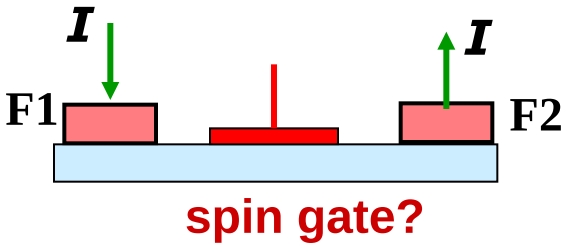

By ?

- Proximity with a ferromagnetic material, magnetic impurity or molecule
- Amplification of spin-orbit by proximity with large S-O material + Electric field or ferroelectric gate
- Edge effects, nanomeshes

Important advantage of graphene: sensitivity of the electronic properties to adatoms, interfaces with magnetic or ferroelectric materials, adsorbed molecules, vacancies, nanomeshes, impurities, strains, geometry of the edges….

Induced spin–orbit splitting in graphene: the role of atomic number of the intercalated metal and π–d hybridization

Alexander M Shikin[1,3], Artem G Rybkin[1], Dmitry Marchenko[1,2], Anna A Rybkina[1], Markus R Scholz[2], Oliver Rader[2] and Andrei Varykhalov[2]

[1] Physics Faculty, St Petersburg State University, ul. Ulyanovskaya 1, 198504 St Petersburg, Peterhof, Russia

[2] Helmholtz-Zentrum Berlin für Materialien und Energie, Elektronenspeicherring BESSY II, Albert-Einstein-Straße 15, D-12489 Berlin, Germany

E-mail: shikin@paloma.spbu.ru

New Journal of Physics **15** (2013) 013016 (18pp)
Received 10 March 2012
Published 9 January 2013
Online at http://www.njp.org/
doi:10.1088/1367-2630/15/1/013016

Abstract. This paper reports spin-dependent valence-band dispersions of graphene synthesized on Ni(111) and subsequently intercalated with monolayers of Au, Cu and Bi. We have previously shown that after intercalation of graphene with Au the dispersion of the π band remains linear in the region of the $\bar{K}$ point of the surface Brillouin zone even though the system exhibits a noticeable hybridization between π states of graphene and d states of Au. We have also demonstrated a giant spin–orbit splitting of π states in Au-intercalated graphene which can reach up to ~100 meV. In this paper we probe in detail dispersions of graphene π–Au d hybridized bands. We show that intercalation of Cu does not produce a noticeable spin–orbit splitting in graphene although this system, similarly to Au-intercalated graphene, also reveals hybridization between graphene states and d states of Cu. To clarify the role of intercalated Au, the electronic and spin structures of Au monolayers on Ni(111) are comparatively studied with and without graphene on top and the importance of the spin splitting of the d states of the intercalated material is established.

PRL 109, 186604 (2012) PHYSICAL REVIEW LETTERS week ending 2 NOVEMBER 2012

Magnetic Moment Formation in Graphene Detected by Scattering of Pure Spin Currents

Kathleen M. McCreary,[1] Adrian G. Swartz,[1] Wei Han,[1] Jaroslav Fabian,[2] and Roland K. Kawakami[1,*]
[1]*Department of Physics and Astronomy, University of California, Riverside, California 92521, USA*
[2]*Institute for Theoretical Physics, University of Regensburg, D-93040 Regensburg, Germany*
(Received 20 July 2012; published 2 November 2012)

Hydrogen adatoms are shown to generate magnetic moments inside single layer graphene. Spin transport measurements on graphene spin valves exhibit a dip in the nonlocal spin signal as a function of the applied magnetic field, which is due to scattering (relaxation) of pure spin currents by exchange coupling to the magnetic moments. Furthermore, Hanle spin precession measurements indicate the presence of an exchange field generated by the magnetic moments. The entire experiment including spin transport is performed in an ultrahigh vacuum chamber, and the characteristic signatures of magnetic moment formation appear only after hydrogen adatoms are introduced. Lattice vacancies also demonstrate similar behavior indicating that the magnetic moment formation originates from p_z-orbital defects.

Topological Frustration in Graphene Nanoflakes: Magnetic Order and Spin Logic Devices

Wei L. Wang,[1] Oleg V. Yazyev,[2,3] Sheng Meng,[1] and Efthimios Kaxiras[1]

[1] *Department of Physics and School of Engineering and Applied Sciences, Harvard University, Cambridge, Massachusetts 02138, USA*
[2] *Ecole Polytechnique Fédérale de Lausanne (EPFL), Institute of Theoretical Physics, CH-1015 Lausanne, Switzerland*
[3] *Institut Romand de Recherche Numérique en Physique des Matériaux (IRRMA), CH-1015 Lausanne, Switzerland*
(Received 13 January 2009; published 13 April 2009)

Magnetic order in graphene-related structures can arise from size effects or from topological frustration. We introduce a rigorous classification scheme for the types of finite graphene structures (nanoflakes) which lead to large net spin or to antiferromagnetic coupling between groups of electron spins. Based on this scheme, we propose specific examples of structures that can serve as the fundamental (NOR and NAND) logic gates for the design of high-density ultrafast spintronic devices. We demonstrate, using *ab initio* electronic structure calculations, that these gates can in principle operate at room temperature with very low and correctable error rates.

Topological Frustration in Graphene Nanoflakes: Magnetic Order and Spin Logic Devices

Wei L. Wang,[1] Oleg V. Yazyev,[2,3] Sheng Meng,[1] and Efthimios Kaxiras[1]

[1]*Department of Physics and School of Engineering and Applied Sciences, Harvard University, Cambridge, Massachusetts 02138, USA*
[2]*Ecole Polytechnique Fédérale de Lausanne (EPFL), Institute of Theoretical Physics, CH-1015 Lausanne, Switzerland*
[3]*Institut Romand de Recherche Numérique en Physique des Matériaux (IRRMA), CH-1015 Lausanne, Switzerland*

(Received 13 January 2009; published 13 April 2009)

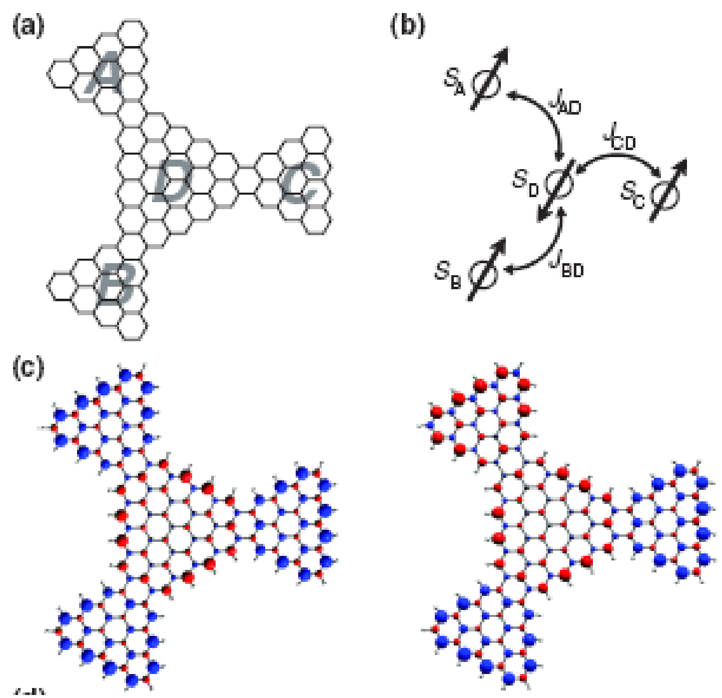

Gate	*A*	*B*	*C*	*D*	E_{tot} (meV)	*D'*	E'_{tot} (meV)
NOR	1	1	1	0	0	1	103
	1	0		0	34	1	68
	0	1		0	34	1	68
	0	0		1	34	0	68
NAND	1	1	0	0	34	1	68
	1	0		1	34	0	68
	0	1		1	34	0	68
	0	0		1	0	0	103

FIG. 4 (color online). (a) Reconfigurable spin logic NOR and NAND gate based on of a tri-bow-tie GNF structure with $n_A = n_B = n_C = 4$, $n_D = 6$, $m = 1$ (A, B, and D are two inputs and one output, respectively, and C is the programming bit). (b) A scheme of the localized spins and the couplings ($2J_{XY} = 34$ meV). (c) Two distinct spin configurations corresponding to 1110 and 0110 for the $ABCD$ spins, respectively. (d) The truth table of the programmable logic gate and the total energy E_{tot} of the operation configuration. D' and E'_{tot} are the error output and the corresponding energy ($E'_{tot} > E_{tot}$).

Giant Nonlocality Near the Dirac Point in Graphene
D. A. Abanin *et al.*
Science **332**, 328 (2011);
DOI: 10.1126/science.1199595

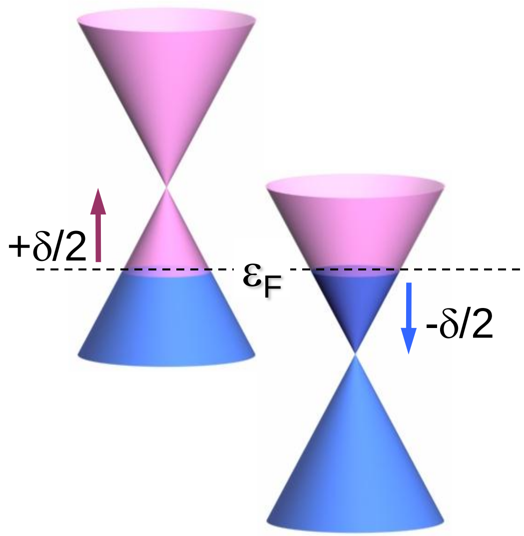

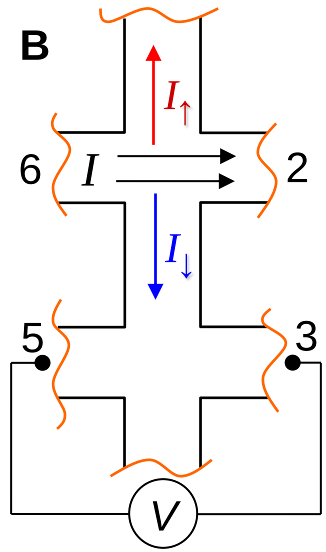

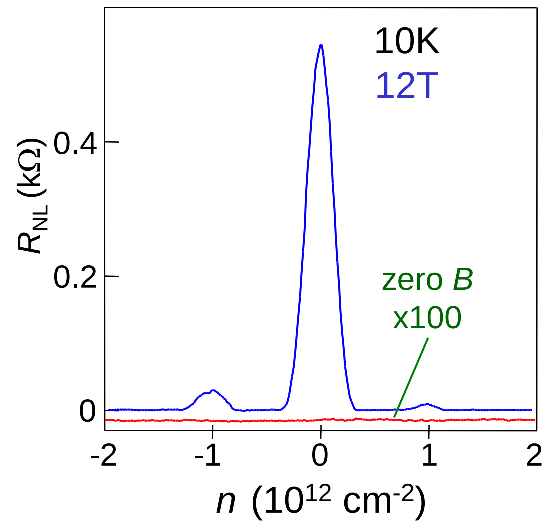

nature physics
LETTERS
PUBLISHED ONLINE: 12 FEBRUARY 2012 | DOI: 10.1038/NPHYS2219

Nonlinear detection of spin currents in graphene with non-magnetic electrodes

Ivan J. Vera-Marun*, Vishal Ranjan and Bart J. van Wees

Spin transport in graphene, examples of previous results

Hill et al, IEEE-TM 2006, Tombros et al, Nature 2007, Cho et al, APL 2007, Ohishi et al, Jap.J.Appl.Phys.2007, Nishioka et al, APL 2007, Goto et al, APL2008, Jozsa et al, PR b 2009, Wang et al, PR B 2008, Han et al, PRL 2010, Yang et al, PRL 2011 and further publications from Groningen, Osaka, Riverside, Singapore, Aachen, etc

First experiments: spin diffusion lengths (< 1 μm) and spin relaxation times were found shorter than expected (from small S-O, weak hyperfine interactions) but, today, begin to increase progressively

Example of recent results: van Wees et al (Groningen), private communication

graphene on BN: spin diffusion length ≈ 6 μm

(longer than in metals or semiconductors
but still small compared to > 20 μm for CNT)

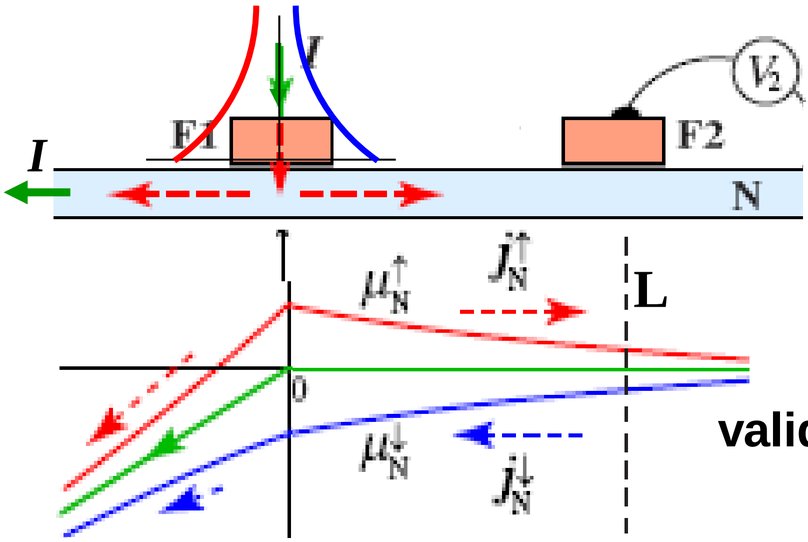

Jedema et al, APL 81, 5162, 2002

$$\frac{V(B_\perp)}{I} = \pm \frac{P^2}{e^2 N(E_F) A} \int_0^\infty \wp(t) \cos(\omega_L t) \exp\left(\frac{-t}{\tau_{sf}}\right) dt.$$

$$\wp(t) = \sqrt{1/4\pi D t} \times \exp(-L^2/4Dt) \tag{4}$$

valid only without spin escape through contacts

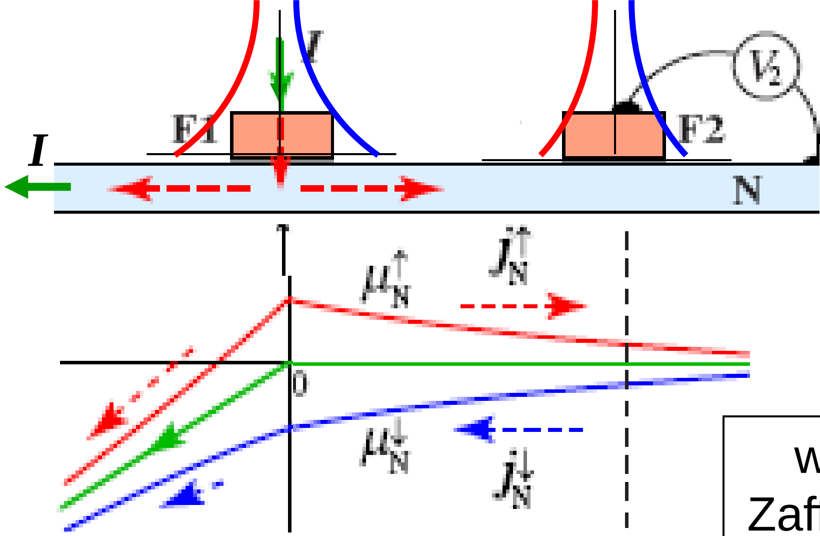

Jedema et al, APL 81, 5162, 2002

$$\frac{V(B_\perp)}{I} = \pm \frac{P^2}{e^2 N(E_F)A} \int_0^\infty \wp(t)\cos(\omega_L t)\exp\left(\frac{-t}{\tau_{sf}}\right) dt. \tag{4}$$

$$\wp(t) = \sqrt{1/4\pi D t} \times \exp(-L^2/4Dt)$$

with spin escape through contacts
Zaffalon and van Wees, PR B71, 2005

An explanation of the above now follows. The first tern proportional to μ_a relaxes the magnetization via two differ ent mechanisms: (a) the interaction of the spin with the nor mal metal (spin-orbit scattering), occurring at a rate τ_{sf}^{-1}, anc (b) the leaking of the spins to the leads, proportional to thi interfaces' conductance, G_j. The time associated with the lat ter is the spin escape time $\tau_{esc} \equiv \Sigma_j G_j (1-P_j^2)/\nu_D e^2 \hat{V}$. Thi total spin-relaxation time is the sum of the two contributions $\tau_{rel}^{-1} = \tau_{sf}^{-1} + \tau_{esc}^{-1}$.

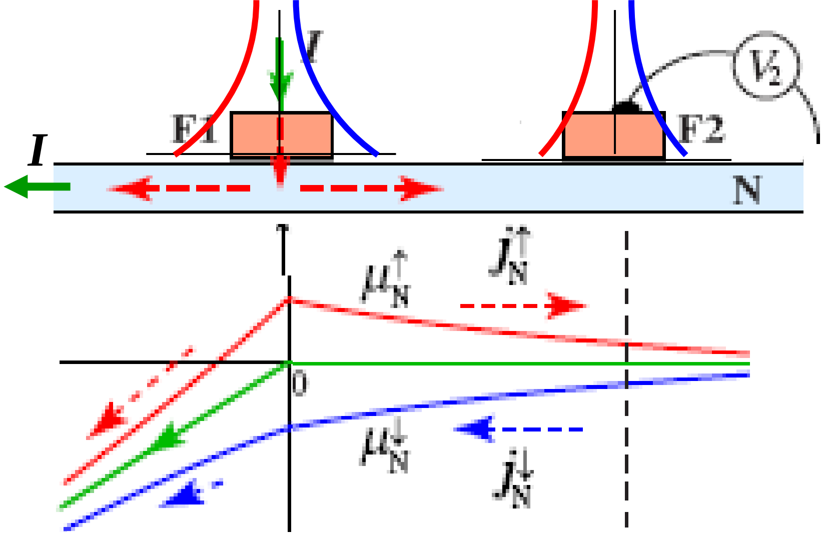

Jedema et al, APL 81, 5162, 2002

$$\frac{V(B_\perp)}{I} = \pm \frac{P^2}{e^2 N(E_F) A} \int_0^\infty \wp(t) \cos(\omega_L t) \exp\left(\frac{-t}{\tau_{sf}}\right) dt.$$

$$\wp(t) = \sqrt{1/4\pi D t} \times \exp(-L^2/4Dt) \quad (4)$$

Fukuma, Otani et al, arXiv 2011

Bohr magneton. For the analysis of the Hanle effect data, the equation (4) in ref. 28 has been widely used but is valid only for LSVs with no spin absorption into the ferromagnetic contact

On the other hand, the equation (1) in this study takes into account the contribution of this spin absorption to the L dependence and the Hanle effects, thus enabling us to analyze ΔR_S in a unified manner[27].

$$\Delta R_S = \frac{4R_N^\omega \left[\frac{P_I}{1-P_I^2}\left(\frac{R_I}{R_N^\omega}\right) + \frac{P_F}{1-P_F^2}\left(\frac{R_F}{R_N^\omega}\right)\right]^2 \left(\frac{\mathrm{Re}\left[\lambda_\omega e^{-L/\lambda_\omega}\right]}{\mathrm{Re}\left[\lambda_\omega\right]}\right)}{\left[1+\frac{2}{1-P_I^2}\left(\frac{R_I}{R_N^\omega}\right)+\frac{2}{1-P_F^2}\left(\frac{R_F}{R_N^\omega}\right)\right]^2 - \left(\frac{\mathrm{Re}\left[\lambda_\omega e^{-L/\lambda_\omega}\right]}{\mathrm{Re}\left[\lambda_\omega\right]}\right)^2}, \quad (1)$$

$$\lambda_\omega = \frac{\lambda_N}{\sqrt{1+i\omega_L \tau_{sf}}}, \quad R_N^\omega = R_N \mathrm{Re}\left[\lambda_\omega / \lambda_N\right]$$

Kawakami et al, 2011

Theoretically, the measured spin lifetime (τ_s) is determined by the spin-flip scattering within the SLG (at a rate of τ_{sf}^{-1}) and spin relaxation induced by the Co contacts. In the latter effect, the spins diffuse into the Co contact with characteristic escape time (τ_{esc}), which limits the measured spin lifetime. For $\lambda_G \rightarrow \infty$, these time scales are simply related by $\tau_s^{-1} = \tau_{sf}^{-1} + \tau_{esc}^{-1}$ [28], while for the more realistic case of finite λ_G, the influence of the contact-induced relaxation should be reduced.

Spin precession and inverted Hanle effect in a semiconductor near a finite-roughness ferromagnetic interface

S.P. Dash, S. Sharma, J.C. Le Breton, J. Peiro, H. Jaffres, J.-M. George, A. Lemaître and R.Jansen (to appear in PR B)

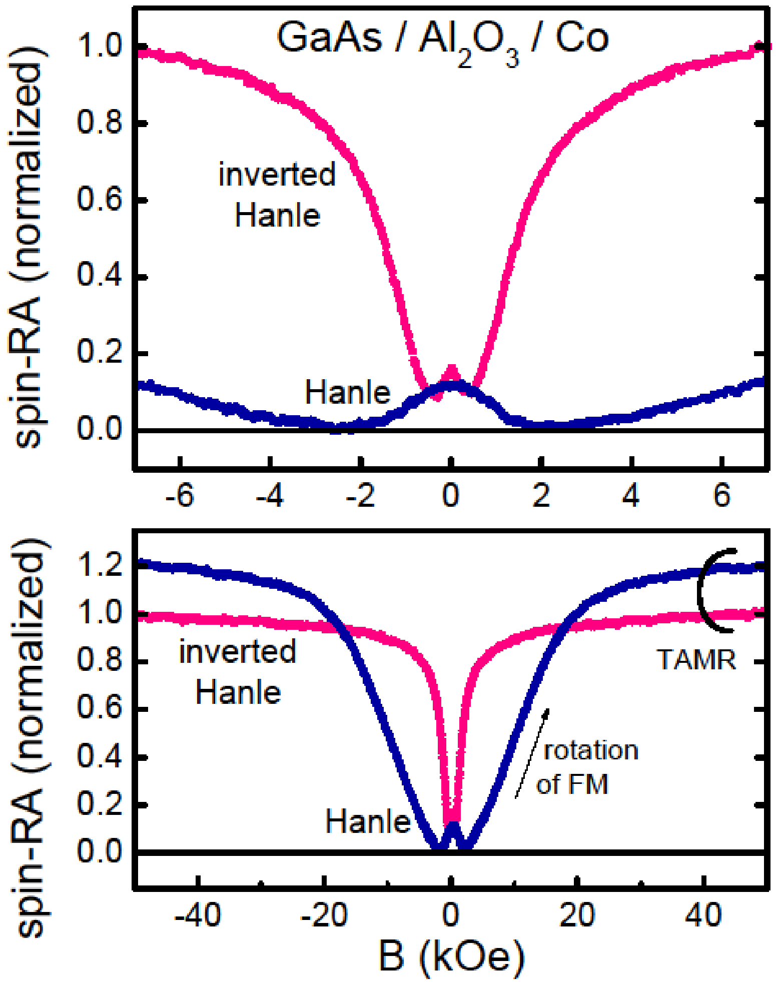

Figure 4 07Apr2011

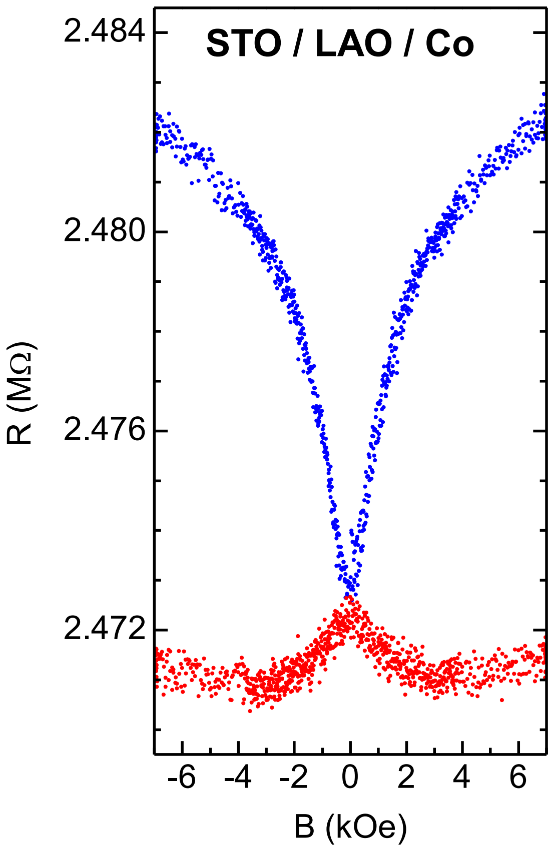
STO / LAO / Co
2.484
2.480
2.476
2.472
R (MΩ)
-6
-4
-2
0
2
4
6
B (kOe)

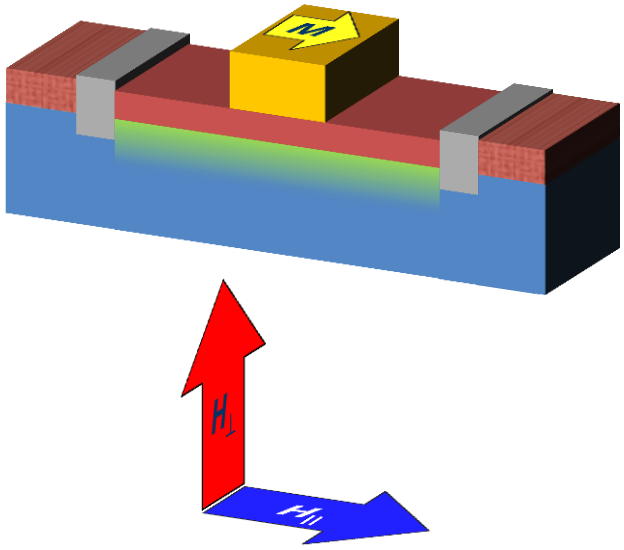
M

Sprinkle et al, arXiv:1001.3869v1,2010

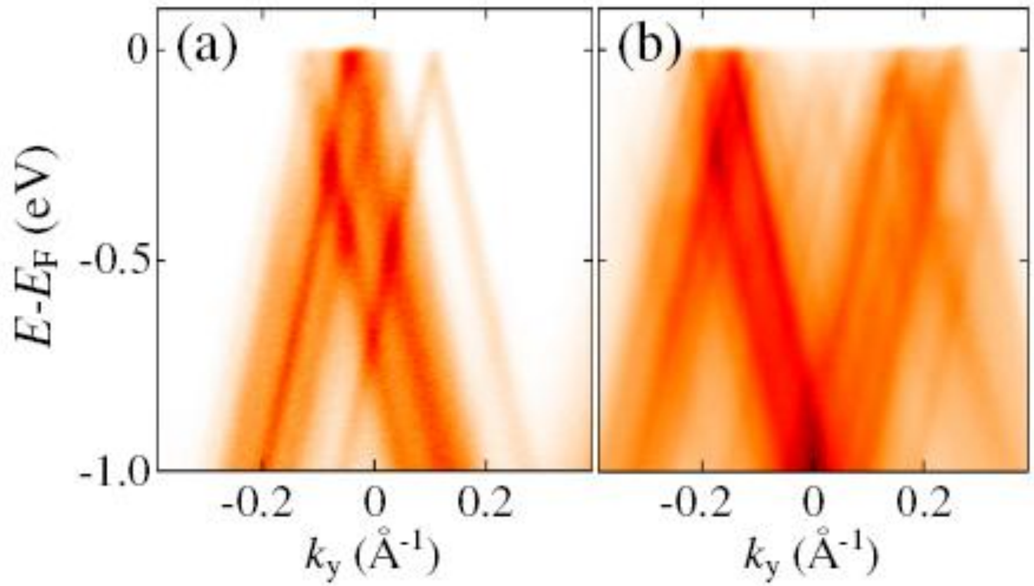

C-face

10 layers

FIG. 10: ARPES scans taken at the K-point radius (k_x = 1.704Å) for a 10-layer grpahene film on the C-face of SiC. The photon energy is 36eV. The scans are taken at two different emission directions: (a) along the SiC $\langle 21\bar{3}0\rangle$ ($\alpha = 0°$) and (b) $\langle 10\bar{1}0\rangle$ ($\alpha = 30°$) directions. The k_y direction is defined in Fig. 7.

Sprinkle et al, arXiv:1001.3869v1, 2010.

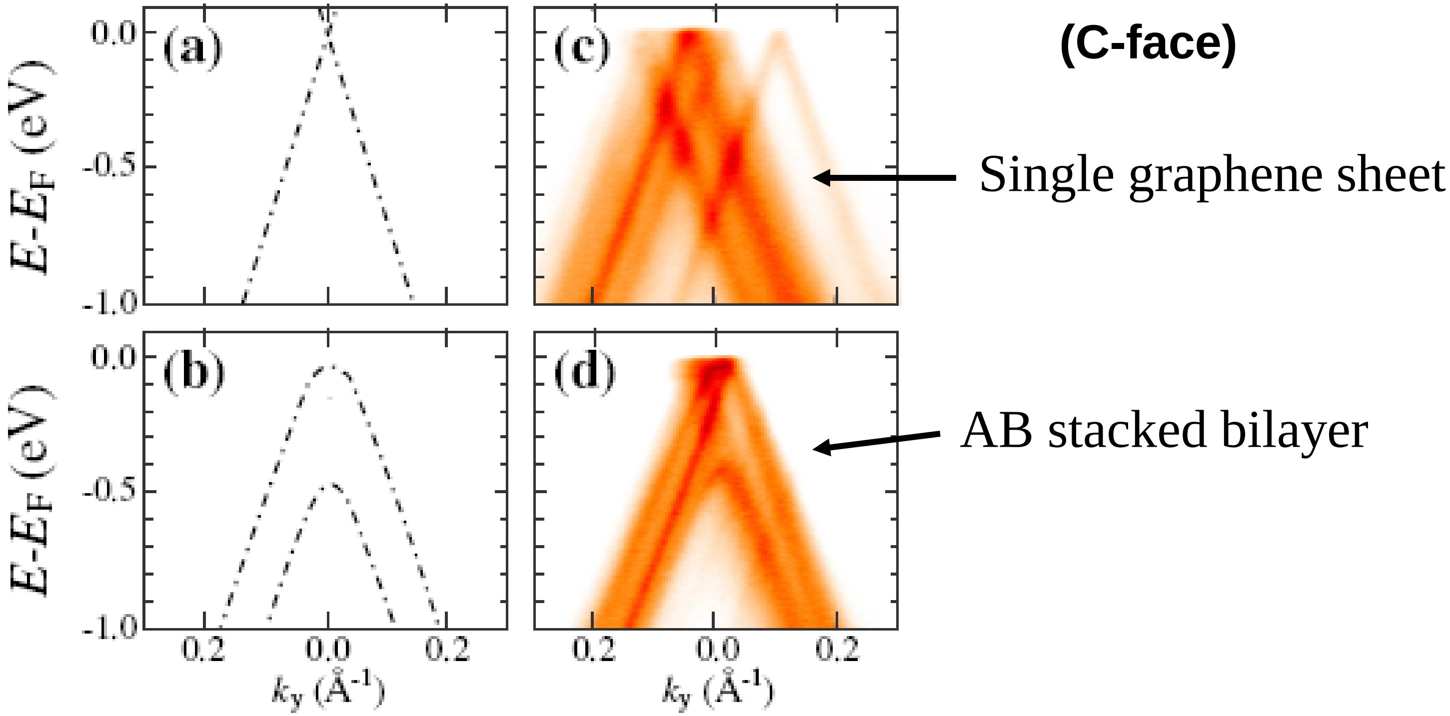

FIG. 16: Comparison of the ARPES band structure near the K-point for a single graphene sheet and an AB bilayer. The calculated tight binding dispersion from both (a) an isolated graphene sheet and (b) the band splitting from an AB stacked bilayer pair are shown. (c) and (d) two experimentally measured bands for multilayered C-face graphene rotated $\phi = 30°$ from the SiC $\langle 21\bar{3}0 \rangle$. (c) shows only linear graphene bands while (d) shows both linear bands and a split band associated with an AB stacked bilayer pair. The photon energy is 36eV and the photon beam size is 40μm.

Spectroscopic Measurement of Interlayer Screening in Multilayer Epitaxial Graphene

Dong Sun,[1] Charles Divin,[1] Claire Berger,[2] Walt A. de Heer,[2] Phillip N. First,[2] and Theodore B. Norris[1,*]

PRL **104,** 136802 (2010)

C-face

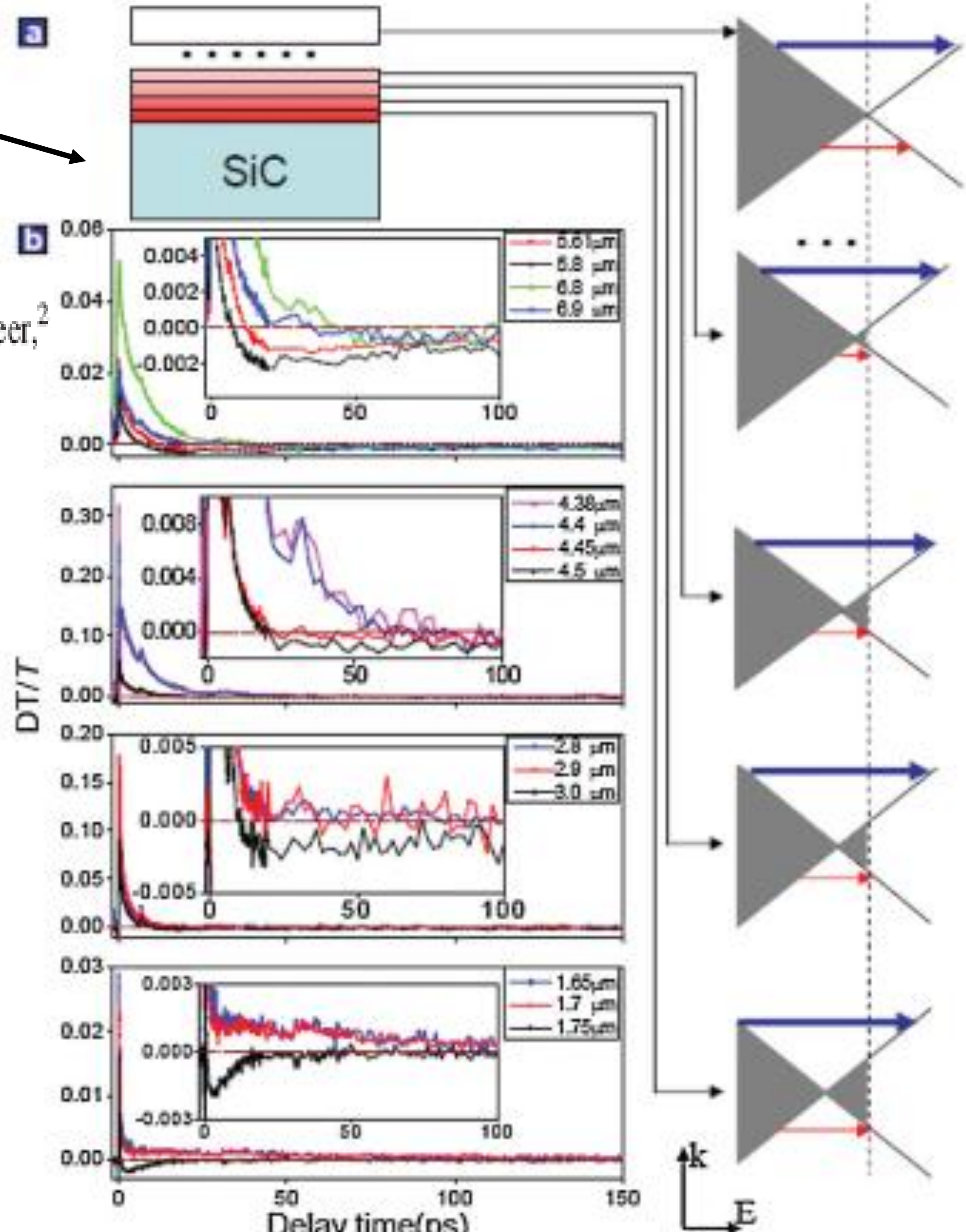

The growth and morphology of epitaxial multilayer graphene

J Hass, W A de Heer and E H Conrad

J. Phys.: Condens. Matter 20 (2008) 323202

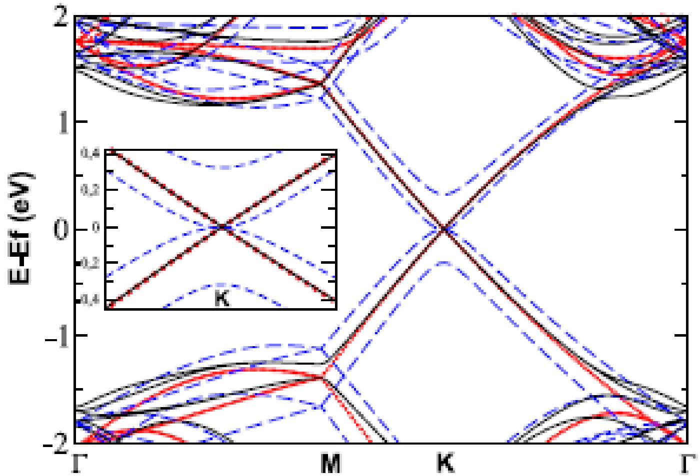

Figure 29. Calculated band structure for three forms of graphene. (i) Isolated graphene sheet (dots), (ii) AB . . . graphene bilayer (dashed line) and (iii) R30/R2$^+$ fault pair (solid line). Inset shows details of band structure at the K-point. Reproduced with permission from [129]. Copyright 2008 by the American Physical Society.

Substrate-induced band gap opening in epitaxial graphene

S.Y. Zhou,[1,2] G.-H. Gweon,[1,*] A.V. Fedorov,[3] P.N. First,[4] W.A. de Heer,[4]
D.-H. Lee,[1] F. Guinea,[5] A.H. Castro Neto,[6] and A. Lanzara[1,2]

ARPES (Si-face)

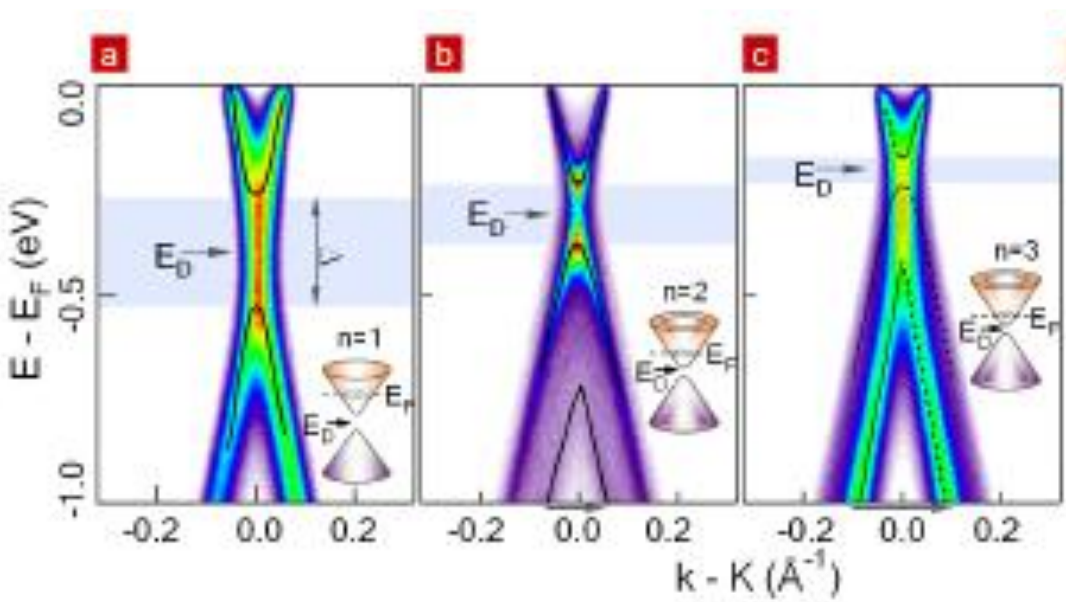

n = 1   n = 2   n = 3

Gap vs n of layers

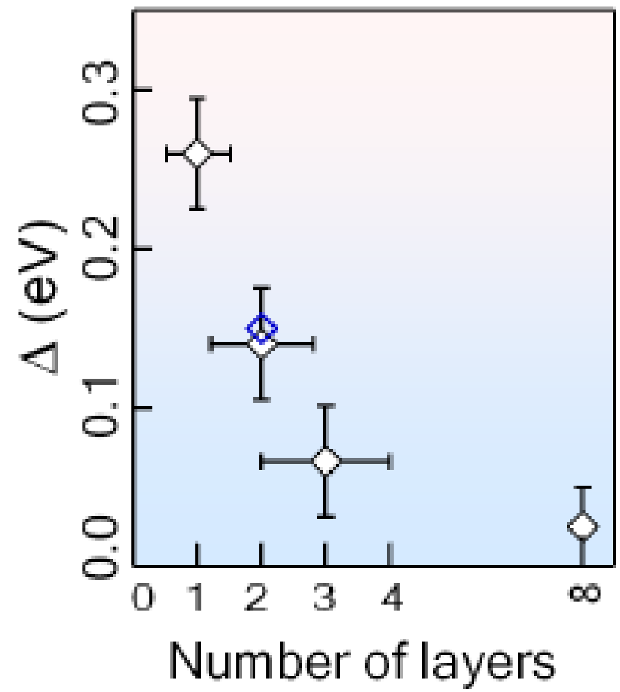

nature physics

ARTICLES

PUBLISHED ONLINE: 3 JUNE 2012 | DOI: 10.1038/NPHYS2331

Highly efficient spin transport in epitaxial graphene on SiC

Bruno Dlubak[1], Marie-Blandine Martin[1], Cyrile Deranlot[1], Bernard Servet[2], Stéphane Xavier[2], Richard Mattana[1], Mike Sprinkle[3], Claire Berger[3,4], Walt A. De Heer[3], Frédéric Petroff[1], Abdelmadjid Anane[1], Pierre Seneor[1]* and Albert Fert[1]

Spin information processing is a possible new paradigm for post-CMOS (complementary metal-oxide semiconductor) electronics and efficient spin propagation over long distances is fundamental to this vision. However, despite several decades of intense research, a suitable platform is still wanting. We report here on highly efficient spin transport in two-terminal polarizer/analyser devices based on high-mobility epitaxial graphene grown on silicon carbide. Taking advantage of high-impedance injecting/detecting tunnel junctions, we show spin transport efficiencies up to 75%, spin signals in the mega-ohm range and spin diffusion lengths exceeding 100 µm. This enables spintronics in complex structures: devices and network architectures relying on spin information processing, well beyond present spintronics applications, can now be foreseen.

Interpretation, determination of spin lifetimes and diffusion lengths

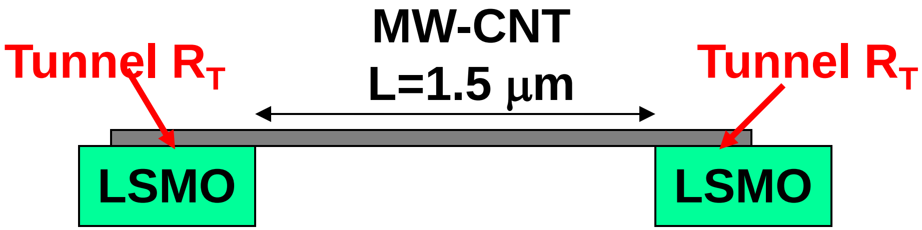

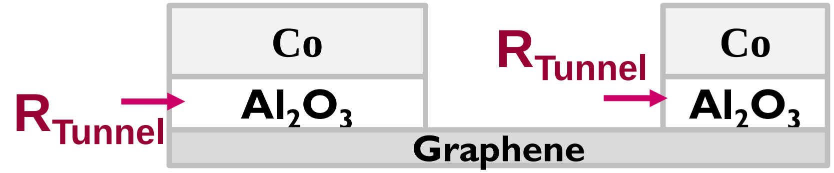

ΔR/R

Too fast spin escape

$$R_T^* << \frac{L}{\lambda_{ch}} R_{ch}^S$$

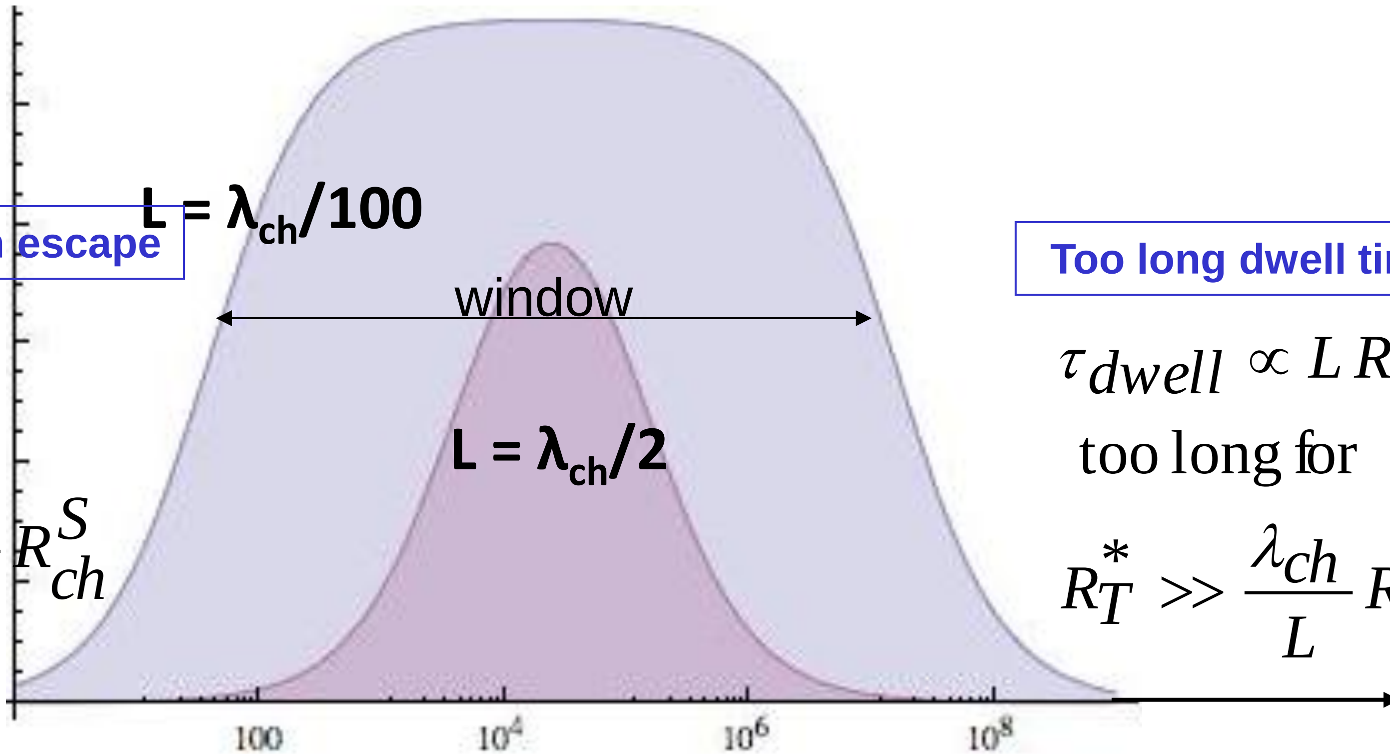

Too long dwell time

$$\tau_{dwell} \propto L\, R_T^*$$

too long for

$$R_T^* >> \frac{\lambda_{ch}}{L} R_{ch}^S$$

R_T^* / R_{ch}^S (interface resistance/spin resistance ratio)

interface ressitance $R_{ch}^S = \rho_{ch}^{\square} \lambda_{ch} / w$